Award Number: W81XWH-12-1-0062

TITLE: Molecular Determinants of Hormone Refractory Prostate Cancer

PRINCIPAL INVESTIGATOR: Atish Choudhury

CONTRACTING ORGANIZATION: Dana-Farber Cancer Institute
Boston, MA 02215

REPORT DATE: July 2017

TYPE OF REPORT: Annual

PREPARED FOR: U.S. Army Medical Research and Materiel Command
Fort Detrick, Maryland 21702-5012

REPORT DOCUMENTATION PAGE

Form Approved
OMB No. 0704-0188

1. REPORT DATE	2. REPORT TYPE	3. DATES COVERED
July 2017	Annual	1 July 2012 - 30 June 2017

4. TITLE AND SUBTITLE
Molecular Determinants of Hormone Refractory Prostate Cancer

5a. CONTRACT NUMBER

5b. GRANT NUMBER
W81XWH-12-1-0062

5c. PROGRAM ELEMENT NUMBER

6. AUTHOR(S)
Atish Choudhury

E-Mail: achoudhury@partners.org

5d. PROJECT NUMBER

5e. TASK NUMBER

5f. WORK UNIT NUMBER

7. PERFORMING ORGANIZATION NAME(S) AND ADDRESS(ES)

Dana-Farber Cancer Institute
450 Brookline Ave
Boston, MA 02215

8. PERFORMING ORGANIZATION REPORT NUMBER

9. SPONSORING / MONITORING AGENCY NAME(S) AND ADDRESS(ES)
U.S. Army Medical Research and Materiel Command
Fort Detrick, Maryland 21702-5012

10. SPONSOR/MONITOR'S ACRONYM(S)

11. SPONSOR/MONITOR'S REPORT NUMBER(S)

12. DISTRIBUTION / AVAILABILITY STATEMENT
Approved for Public Release; Distribution Unlimited

13. SUPPLEMENTARY NOTES

14. ABSTRACT

We have performed a high throughput, *in vivo* genetic screen to identify kinases that permit androgen-dependent transformed prostate epithelial cells (LHSR-AR cells) to form tumors in female animals. In addition to known prostate cancer oncogenes and mediators of androgen independence (mutated KRAS, constitutively active MEK, RAF1, ERBB2, AKT1, PIM1 and PIM2), overexpression of the Never In Mitosis A (NIMA) related kinase 6 (NEK6) reproducibly yielded androgen-independent tumors. NEK6 is overexpressed in prostate cancer cell lines compared to their normal counterparts and is overexpressed in a subset of human prostate cancers. Expression of NEK6 confers castration resistance to established tumors in male mice, and suppressing NEK6 expression restores sensitivity to castration. Castration-resistant tumors generated through NEK6 overexpression are predominantly squamous in histology and AR negative. Phosphoproteome analysis reveals the transcription factor FOXJ2 to be a novel substrate. The gene expression profile mediated by NEK6 overexpression in tumors from castrated mice demonstrates elements of both differentiation and immune signaling, and a phosphomimetic form of FOXJ2 leads to transcriptions of newly identified NEK6 transcriptional targets. These studies reveal a novel mechanism of resistance in androgen pathway independent prostate cancer (APIPC). Analysis of a genome-wide ORF screen for genes conferring androgen-independent proliferation of LNCaP cells *in vitro* suggests CREB5 as a novel mediator of castration resistance.

15. SUBJECT TERMS
Prostate cancer, hormone refractory, castration resistant, androgen independent, NEK6

16. SECURITY CLASSIFICATION OF:			17. LIMITATION OF ABSTRACT	18. NUMBER OF PAGES	19a. NAME OF RESPONSIBLE PERSON
a. REPORT	b. ABSTRACT	c. THIS PAGE			USAMRMC
U	U	U	UU	44	19b. TELEPHONE NUMBER *(include area code)*

Table of Contents

INTRODUCTION

We have performed a high throughput, in vivo genetic screen to identify kinases that permit androgen-dependent transformed prostate epithelial cells (LHSR-AR cells) to form tumors in female animals. In addition to known prostate cancer oncogenes and mediators of androgen independence (mutated KRAS, constitutively active MEK, RAF1, ERBB2, AKT1, PIM1 and PIM2), overexpression of the Never In Mitosis A (NIMA) related kinase 6 (NEK6) reproducibly yielded androgen-independent tumors. NEK6 is overexpressed in prostate cancer cell lines compared to their normal counterparts and is overexpressed in a subset of human prostate cancers. Expression of NEK6 confers castration resistance to established tumors in male mice, and suppressing NEK6 expression restores sensitivity to castration. Castration-resistant tumors generated through NEK6 overexpression are predominantly squamous in histology and AR negative. Phosphoproteome analysis reveals the transcription factor FOXJ2 to be a novel substrate. The gene expression profile mediated by NEK6 overexpression in tumors from castrated mice demonstrates elements of both differentiation and immune signaling, and a phosphomimetic form of FOXJ2 leads to transcriptions of newly identified NEK6 transcriptional targets. These studies reveal a novel mechanism of resistance in androgen pathway independent prostate cancer (APIPC). Analysis of a genome-wide ORF screen for genes conferring androgen-independent proliferation of LNCaP cells in vitro suggests CREB5 as a novel mediator of castration resistance.

BODY

Background

Prostate cancer is the third most common cause of cancer death in men, and the majority of these deaths occur in patients with metastatic castration-resistant prostate cancer (CRPC). Clinical responses to agents that decrease circulating androgens to below castrate levels (abiraterone – Attard *et al.*, 2009) and new potent antagonists of the androgen receptor (enzalutamide – Scher *et al*., 2012) demonstrate that the androgen receptor (AR) signaling pathway remains critical in CRPC. Recent reports from studies of metastatic tissue in patients who have progressed on these therapies reveal that tumors can become resistant either through persistent activation of the AR pathway, or by progression to a state described as androgen pathway independent prostate cancer (APIPC) (Nelson, 2012), with or without evidence for neuroendocrine transdifferentiation.

Constitutive activation of kinases such as ERBB2, MAPK, PI3K/Akt, and Src [1-4] has been implicated in mediating resistance to hormonal therapies through both AR-dependent [5-7], and AR-independent mechanisms [8]. A number of recent studies have demonstrated the complementarity and crosstalk between kinase signaling pathways and AR signaling. Mendiratta, *et al*. (2009) developed a gene expression signature of AR signaling, and found that decreased predicted AR activity in patient samples correlated with increased predicted Src activity. Carver, *et al*. (2011) and Mulholland, *et al*. (2011) demonstrated cross-regulation through reciprocal feedback between the AR and PTEN/PI3K/MTOR signaling pathways. However, inhibitors of many of these kinases have failed to demonstrate significant clinical benefit in unselected patient populations, such as in trials of the ERBB2 inhibitor lapatinib (Whang *et al*., 2011), the MTOR inhibitor everolimus (Nakabayashi *et al*., 2012), and the SRC inhibitor dasatinib (Araujo *et al*., 2013). An agent targeting MET and VEGFR2, cabozantinib, has demonstrated interesting clinical activity in metastatic CRPC (Smith *et al*., 2014), but has not demonstrated improvements in overall survival or bone pain in randomized phase III trials.

Tumor samples from patients with CRPC have increased levels of tyrosine phosphorylation as compared to treatment naïve prostate cancer (Drake, *et al*. 2012; Drake *et al.,* 2013), and analysis of serine/threonine and tyrosine phosphorylation events in metastatic CRPC suggests particular signaling networks involved in this transition (Yazdi, *et al*. 2014). However, there is limited evidence for activating kinase point mutations in CRPC, suggesting that kinase pathways are activated by other (structural genetic, epigenetic, microenvironmental) mechanisms. Kinase signaling pathways whose activation could lead to castration resistance in patients have not been comprehensively catalogued, so we have performed an *in vivo* functional genomic screen to identify novel pathways that may be involved. These studies would help identify novel targets for therapeutic intervention (either the kinases themselves, or upstream/downstream mediators) and help with biomarker development for stratifying patients for likelihood of response to therapy.

We hypothesize that novel signaling pathways may be involved in conferring castrate resistance, and given that kinases usually act as transducers of growth and proliferation signals, we hypothesize more specifically that activated/amplified kinases play a role in the development of castration resistance. We have thus performed an *in vivo* functional genomic screen to identify novel pathways that may be involved and likely serve as therapeutic targets in these patients.

Previous work in our laboratory (Berger *et al*., 2004) demonstrated that primary prostate epithelial cells (PrECs) that are rendered tumorigenic by the expression of the SV40 large T and small t antigens, the catalytic subunit of telomerase (hTERT), H-Ras, and the androgen receptor (LHSR-AR cells) form well-differentiated tumors in mice. These tumors are androgen-dependent and are thus unable to grow in female or castrated mice. I have performed a high throughput, *in vivo* genetic screen to identify kinases that permitted these cells to form tumors in female animals. A lentivirally delivered kinase ORF library encompassing 601 kinases and other oncogenes was introduced into these cells in pools of 9-10, and I identified fourteen ORF integrants that allowed for the androgen-independent development of subcutaneous tumors by PCR using vector specific primers (Table 1). Using the same ORF library, I performed an *in vitro* screen for genes conferring androgen-independent proliferation to androgen dependent LNCaP cells and identified 13 genes that significantly (>2 standard deviations from median) increased proliferation in androgen-deprived conditions (Table 1).

The 24 total candidates identified from both screens were introduced into LHSR-AR cells individually and injected into 6 subcutaneous sites of female BALB/C nude mice for validation of androgen-independent tumor formation. Among the candidates that reproducibly yield androgen-independent tumors are mutated KRAS; RAF1, which is recurrently translocated (Palanisamy *et al*. 2010) and amplified (Taylor *et al*., 2010) in advanced prostate cancer; ERBB2, AKT1, and constitutively active MEK1, which have been implicated in androgen independence ([1-4]; and PIM1 and PIM2, which have previously been demonstrated to be important oncogenes in prostate cancer (Brault *et al*., 2010). Among the strongest candidates identified to confer androgen independence in this assay are the Never In Mitosis A (NIMA) related kinase 6 (NEK6), and nemo-like kinase (NLK).

Aim 1. Elucidating the role of NIMA-related kinase 6 (NEK6) and nemo-like kinase (NLK) as mediators of castrate-resistant prostate cancer and assessing their potential as therapeutic targets.

Milestone 1: Determine whether NEK6 and NLK can confer castrate resistance to established tumors, whether kinase activity is required, and whether their continued expression is required.

In addition to conferring tumor formation in female mice, overexpression of NEK6 in LHSR-AR cells also lead to tumor formation in castrated mice, which lack circulating androgens since mice do not synthesize androgens from their adrenal glands (Figure 1A). The tumors in castrated mice are generally smaller and slower growing than those in female mice, suggesting that signaling mediated by androgens play a role in the growth of the tumors even though they are not essential for tumor formation. In addition, we tested whether NEK6 overexpression can lead to androgen-independent tumor formation in a different genetic context, that is in immortalized PrECs transformed by overexpression of the MYC oncogene and expression of an active form of the p110α subunit of PI3 kinase (rather than with small t antigen and active HRAS), termed LHMK-AR cells. Indeed, NEK6 overexpression led to tumor formation in this other genetic context (Figure 1B); however given that the tumors were smaller and somewhat less robust than those formed from LHSR-AR cells, functional studies performed below focused on tumors formed from the latter cells.

Table 1. Results of *in vivo* and *in vitro* screens for genes conferring androgen independence, and of *in vivo* validation.

In vivo LHSR-AR screen		*In vitro* LNCaP screen		*In vivo* validation	
ORF	# tumors	ORF	Fold proliferation (× median)[b]	ORF	# tumors
KRASV12+MEKDD[a]	3/3	**NLK**	2.09	KRASV12	6/6
ERBB2	3/3	CDK6	1.90	ERBB2	5/6
NEK6	3/3	PIM1	1.72	**NEK6**	5/6
RAF1	3/3	CDK4	1.55	**NLK**	4/6
AKT1	1/3	PIM2	1.45	MEKDD	4/6
BRD3+NEK8[a]	1/3	STK40	1.44	AKT1	3/6
PIM2	1/3	RPS6KA2	1.40	RAF1	3/6
GK	1/3	AGK	1.40	PIM1	3/6
PFKP	1/3	TGFBR1	1.40	PIM2	1/6
PRKG2	1/3	DAPK3	1.39	others	0/6
TGFBR2	1/3	LOC389599	1.38		
PIM1	1/3	NEK5	1.37		
		AKT1	1.37		

[a] Two ORF integrants were amplified from these tumors
[b] For reference, the synthetic androgen R1881 leads to median 2.06 fold proliferation

The kinase activity of NEK6 is required for castration-resistant tumor formation, as a kinase dead version with mutations of lysine residues at amino acids 74 and 75 to methionine (K74M/K75M) did not confer this phenotype (Supplemental Figure S1A). To assess whether NEK6 could serve

as a therapeutic target in established tumors where its activity is increased, we implanted cells with doxycycline-inducible expression of NEK6 (Figure 1C) in male mice with a testosterone pellet, and tumors were allowed to form in the presence of doxycycline in the diet. After 35 days, the mice were castrated, testosterone pellets was removed, and doxycycline was either continued or withdrawn (5 mice = 15 tumors per group; mice that died perioperatively were excluded from the analysis). We found that at day 30 after castration NEK6 confers resistance to castration compared to the parental cells when its expression is maintained with doxycycline ($p=0.001$) but sensitivity to castration is restored when doxycycline is withdrawn ($p=0.049$) (Figure 1C).

The tumors formed due to NEK6 overexpression have regions of nuclear AR expression but the majority of these tumors lacked AR expression (Figure 2A). Hematoxylin and eosin (H&E) staining demonstrates squamous differentiation in these tumors with the more mature differentiated regions demonstrating keratin deposition and AR loss. Androgen-independent tumors derived from expression of the other kinases identified in the screen also have regions of AR-positivity and negativity that vary in proportion and intensity (Supplemental Table S1). NEK6 overexpressing tumors established in male mice demonstrate strong nuclear AR staining with no squamous differentiation (Figure 2B, left panels). However, after castration, these tumors lose nuclear AR over time and develop more keratinization between nests of tumor cells (Figure 2B, bottom panels). This observation suggests that NEK6-mediated castration resistance does not require AR activity, and that transdifferentiation to a squamous phenotype is a result of or response to castration.

Milestone 1: NEK6 can confer castrate resistance to established tumors, kinase activity is required, and continued expression is required. The NEK6-mediated castration-resistant tumors are AR negative and squamous in histology.

Aim 2: Assessing signaling pathways involved in NEK6 and NLK-mediated castrate resistance and assessing their clinical relevance.

Milestone 2: Determine whether AR and STAT3 are necessary to confer NEK6 and NLK-mediated castrate resistance

Milestone 3: Determine impact of NEK6 and NLK on AR and STAT3 compared to other hits in the screen in vitro and in vivo

Given that persistence of AR signaling has been demonstrated to be an important mechanism of castration resistance, we sought to determine if NEK6 influences AR signaling. As noted previously, the NEK6-mediated castration resistant tumors lack expression of the AR, making it unlikely that AR is responsible for this phenotype. NEK6 overexpression does not lead to an increase in activity of an AR reporter based on the PSA enhancer in LNCaP cells (Supplemental Figure S3A), and inducible overexpression of NEK6 in LHSR-AR cells (Supplemental Figure S3B) does not lead to increased expression of the AR targets PSA and TMPRSS2 (Supplemental Figure S3C). Gene set enrichment analysis (Subramanian *et al*., 2005) of an mRNA expression signature of NEK6 activity generated from cells inducibly expressing wild-type vs. a kinase dead NEK6 form of NEK6 (with lysine resides at positions 74 and 75 mutated to methionine – O'Regan and Fry, 2009) *in vitro* demonstrates that gene expression changes associated with NEK6 kinase activity do not correlate positively or negatively (Supplemental Figure S3D) with three previously published signatures of AR activity (Hieronymus *et al*., 2006; Mendiratta *et al*., 2009; Sharma *et al.,* 2013).

It has previously been demonstrated that xenograft tumors with squamous histology can also be generated by transformation of patient-derived prostate basal cells (Stoyanova *et al*., 2013) with these tumors marked by active β-catenin; however there is no evidence for nuclear β-catenin staining in the NEK6-mediated castration resistant tumors generated here (Supplemental Figure S4A). Thus, we sought to determine whether other canonical oncogenic signaling pathways previously reported to be activated by NEK6 may be playing a role. NEK6 purified from rat liver was found to be the major protein kinase that is active on the p70 S6 kinase (RPS6KB1) hydrophobic regulatory site, Thr412 (Belham *et al*., 2001). Subsequently, it was demonstrated that NEK6 could phosphorylate hydrophobic motifs of RPS6KB1 as well as SGK1 *in vitro* (Lizcano *et al*., 2002). In addition, STAT3 phosphorylation at serine 727 has been implicated in the transformation activity of NEK6 previously (Jeon *et al*., 2010). However, inducible expression of NEK6 in LHSR-AR cells does not increase phosphorylation on RPS6KB1 at Thr412 or STAT3 at Ser727 with or without growth factor stimulation as compared to cells expressing kinase-dead NEK6 or GFP (Supplemental Figure S4B). We were not able to find a quality antibody recognizing Ser422 of SGK1, but we were unable to demonstrate phosphorylation of SGK1 at Ser422 by active recombinant NEK6 in an *in vitro* kinase assay (data not shown).

Because NEK6 has previously been described to play a role in the G2/M transition (Yin *et al*., 2003) with its proliferative effects in hepatocellular carcinoma reported to be mediated through modulation of cyclin B (Zhang *et al*., 2014), we assessed whether NEK6 overexpression can influence cell cycle progression in our system. The baseline cell cycle profile is identical for cells with inducible expression of NEK6 with and without doxycycline in normally cycling cells, cells starved in growth-factor free media, and in cells released into growth-factor containing media (Supplemental Figure S5A). NEK6 does not increase proliferation rate of LHSR-AR cells *in vitro* compared to a lacZ control (Supplemental Figure S5B). Thus, the functional role of NEK6 overexpression in these cells does not appear to be related to cell cycle progression. Another activity of NEK6 that has been implicated in its oncogenic activity is inhibition of p53-mediated senescence (Jee *et al*., 2010). LHSR-AR cells express large-T antigen, so the p53 pathway should be inactive in these cells. To confirm this in our multiply infected LHSR-AR cells, they were exposed to etoposide at 10 μM for 18 hours or 50 μM for 4 hours: under neither condition is p21 expression induced, while the level of cleaved PARP is not altered by NEK6 expression (Supplemental Figure S5C). Thus NEK6 does not act by modulating the p53 pathway, and furthermore the pro-survival effect of NEK6 appears to be specific to the *in vivo* context of castration resistance.

Milestones 2 and 3: NEK6 does not activate AR signaling and does not lead to detectable STAT3 phosphorylation in LHSR-AR cells. In addition, there is no evidence that NEK6 activates beta-catenin or RPS6KB1 signaling, promotes cell cycle progression, or antagonizes p53 signaling in our model.

Milestone 4: Generation of mRNA and phosphoproteomic signatures corresponding to androgen independence conferred by our hits, and comparison to androgen signaling and existing databases

Identification of FOXJ2 and NCOA5 as NEK6 substrates

To gain a more comprehensive understanding of the immediate signaling mediated by NEK6 expression and discover novel *in vivo* substrates, we performed a phosphoproteomic analysis. Constructs for the expression of wild-type and kinase-dead NEK6 under the control of a doxycycline-inducible promoter were introduced into LHSR-AR cells, and we created phosphoproteomic profiles of cells expressing doxycycline inducible versions of: (1) wild-type NEK6 in the presence of doxycycline, (2) kinase-dead NEK6 in the presence of doxycycline, and (3) wild type NEK6 without doxycycline. Cells were cultured in "light", "medium", and "heavy" media for Stable Isotope Labeling by Amino acids in Cell culture (SILAC) for 7 days in 2 different permutations; they were growth factor starved for the final 30 hours and then growth factor stimulated for 5 minutes. Lysates were then subjected to SCX-IMAC phosphorylation analysis and assayed by mass spectrometry.

A total of 9418 phosphopeptides (8432 phosphoserine, 952 phosphothreonine, 34 phosphotyrosine) from 3401 proteins were detected in this experiment. 59 phosphopeptides from 50 proteins were increased in both the wild-type induced vs. un-induced and wild-type vs. kinase dead comparison with a combined q value of <0.25 (Supplemental Table S4). The differentially phosphorylated proteins include a large number of transcriptional regulators, including the forkhead-box family proteins FOXO3 and FOXA1, and the phosphopeptides represent a variety of common phophorylation motifs as shown in Figure 5A. Among these motifs are pS/pT-P, associated with MAPK/CDK/GSK3 signaling, and R-X-R-X-X-pS/pT, associated with AKT and RSK (ribosomal S6-kinase) signaling. We noted that the frequency of these motifs among the 59 differential phosphopeptides is not increased as compared to their frequency among all detected phosphopeptides - for example, pS/pT-P motifs were found in 26 of the 59 differential phosphopeptides vs. 4815 of the 9434 total phosphopeptides (44% vs. 51%, p=NS). This suggests that NEK6 does not globally activate MAPK/CDK/GSK3, AKT/RSK, CAMK or CK2 signaling.

However, a canonical NEK6 motif (Vaz Meirelles *et al*., 2010) with leucine at the -3 position [L-X-X-pS/pT-F/W/Y/M/L/I/V/R/K] is more frequently represented in the 59 significantly enriched phosphopeptides compared to all detected phosphopeptides (p=0.0092 Fisher's exact); an "acceptable" NEK6 substrate motif [L/F/W/Y-X-X-pS/pT-F/W/Y/M/L/I/V/R/K] is even more significantly enriched ($p=1.95\times10^{-5}$). This suggests that this peptide sequence is a true description of the NEK6 phosphorylation motif, and that the 8 proteins with phosphopeptides of this form detected here (FOXJ2, HUWE1, NCOA5, KRT18, TRA2B, HNRNPM, HNRNPA2B1, ZNF326) are bona fide *in vivo* NEK6 substrates.

To confirm whether detection of these phosphopeptides in cells is due to direct phosphorylation by NEK6, we assessed the activity of commercially available recombinant GST-NEK6 on a subset of these proteins immunoprecipitated via a C-terminal V5-tag through an on-bead kinase assay. We initially focused on the transcription factors FOXJ2 and NCOA5 because they are related to families of transcription factors already described to be important in prostate cancer

(Tao, *et al*., 2014; Qin *et al*., 2014). We were able to confirm phosphorylation of FOXJ2 and NCOA5, with no phosphorylation of a lacZ control (Figure 5B). Mutation of the phosphorylation sites of FOXJ2 and NCOA5 identified via mass spectrometry, Ser8 and Ser96 respectively, decreases the *in vitro* phosphorylation of these substrates, demonstrating the specificity of the kinase activity at these residues.

Mapping NEK6 phosphorylation sites on FOXJ2 and NCOA5

To comprehensively map the phosphorylation sites of NEK6 on FOXJ2 and NCOA5, all serine and threonine residues in these proteins in "acceptable" NEK6 phosphorylation motifs as described above [L/F/W/Y-X-X-pS/pT-F/W/Y/M/L/I/V/R/K] were identified; when the relevant serines and threonines are mutated to aspartic acid, the resulting mutant forms of these proteins are phosphorylated significantly less than the wild type counterpart (compare lanes 2 and 1 in right panels of Figures 6A and B). When mutating all of these potential phosphorylation sites but maintaining one of the serines/threonines as wild type, it is apparent that NEK6 can phosphorylate FOXJ2 at Thr23 and Ser254 (Figure 6A, lanes 3 and 5) in addition to Ser8; NCOA5 at Ser21 and Ser151 (Figure 6B, lanes 3 and 4) in addition to Ser96. The phosphorylation of FOXJ2 and NCOA5 *in vitro* is indeed due to the active GST-NEK6 added to the assay as excluding it led to no detectable phosphorylation of these substrates (Figure 6C lanes 2 and 6).

Gene Expression changes mediated by NEK6

Since the observed castration resistance mediated by NEK6 does not appear to involve these previously described pathways, we sought to elucidate downstream signaling mediated by NEK6 overexpression in an unbiased manner by examining gene expression changes in NEK6 driven tumors under castrate conditions. We established subcutaneous tumors in male mice with LHSR-AR cells expressing NEK6 under a doxycycline-inducible promoter; after tumors formed, 7 days before planned tumor harvest we split the mice into two groups, with half continuing on doxycycline diet and half discontinuing doxycycline. We then castrated the animals and harvested the tumors at days 0, 2 and 5 after castration. We found that doxycycline withdrawal reduced NEK6 levels to baseline (Figure 4A). We then analyzed gene expression by RNA-Seq on mRNA isolated from tumors harvested from mice with and without doxycycline in their diet at days 2 and day 5 after castration (3 tumors under each condition, 12 samples total).

To characterize gene expression changes associated with NEK6 expression in response to castration, we performed GSEA comparing tumors overexpressing NEK6 (+dox) at day 5 after castration with –dox controls (Figure 4B). The top two curated gene sets from the molecular signatures database (MSigDB collection C2, representing 4725 gene sets) correlated with the NEK6 signature are (i) genes down-regulated in primary B lymphocytes within 60-180 min after activation of LMP1, an oncogene encoded by Epstein-Barr virus (Dirmeier *et al*, 2005) and (ii) genes representing the epithelial differentiation module in sputum during asthma exacerbations (Bosco, *et al*., 2010). The GO biological process most significantly enriched among the NEK6-upregulated genes as assessed using the Gene Ontology for Functional Analysis (GOFFA) software (Sun *et al*., 2006) was "response to biotic stimulus" (p=0.0005) (Supplemental Table S2); other relevant terms include "apoptotic signaling pathway" (p=0.0056), "cytoskeleton organization" (p=0.0084), cytokine-mediated signaling pathway (p=0.0085) and "epithelial cell differentiation" (p=0.0183). One of these differentiation genes is cytokeratin 13 (KRT13), a known marker of squamous differentiation in the literature (van Dorst *et al*., 1998). KRT13 expression in xenograft tumors expressing NEK6 in the presence of circulating androgens is modest (Supplemental Figure S6, left panels), but increases with castration preferentially in tumors that continue to express NEK6 under a doxycycline inducible promoter as compared to tumors where NEK6 expression is abrogated by doxycycline withdrawal (Supplemental Figure S6, right panels).

We hypothesized that NEK6 may mediate resistance to castration in tumors by maintaining survival signaling that is lost when AR is no longer activated by circulating androgens. To understand components of this survival signaling, we compared gene expression of control tumors (i.e. without NEK6 overexpression) at the day 2 and day 5 time points. We found that the top gene set and six of the top 12 gene sets by GSEA associated with gene expression lost following castration reflected interferon signaling (Table 3). In addition, two prostate cancer related gene sets were also highly correlated with genes downregulated by castration (ranked 9 and 12): genes up-regulated in prostate tumors developed by transgenic mice overexpressing Vav3 (Liu *et al.,* 2008) and genes up-regulated in prostate cancer samples from African-American patients compared to those from the European-American patients (Wallace *et al*., 2008). These latter signatures were reported to incorporate elements of NFκB signaling and interferon signaling respectively, suggesting that the loss of circulating androgens leads to a decrease in immune-type signaling in these tumors.

Table 3. Gene sets enriched in ranked list of genes with decreased expression after castration (Control Day 5 vs. Day 2)

	GS	SIZE	ES	NES	NOM p-val	FDR q-val	FWER p-val
1	REACTOME_INTERFERON_ALPHA_BETA_SIGNALING	46	0.69	3.2	0	0	0
2	LIANG_SILENCED_BY_METHYLATION_2	44	0.64	3.04	0	0	0.001
3	BOWIE_RESPONSE_TO_TAMOXIFEN	17	0.82	3	0	0.001	0.003
4	BROWNE_INTERFERON_RESPONSIVE_GENES	61	0.6	2.98	0	0.001	0.005
5	ZHANG_INTERFERON_RESPONSE	20	0.78	2.98	0	0.001	0.005
6	BOWIE_RESPONSE_TO_EXTRACELLULAR_MATRIX	16	0.8	2.97	0	0.001	0.009
7	MOSERLE_IFNA_RESPONSE	30	0.68	2.93	0	0.002	0.013
8	SANA_TNF_SIGNALING_UP	71	0.56	2.92	0	0.002	0.016
9	LIU_VAV3_PROSTATE_CARCINOGENESIS_UP	59	0.57	2.88	0	0.003	0.023
10	DER_IFN_ALPHA_RESPONSE_UP	69	0.55	2.88	0	0.002	0.023
11	SANA_RESPONSE_TO_IFNG_UP	60	0.57	2.84	0	0.003	0.037
12	WALLACE_PROSTATE_CANCER_RACE_UP	168	0.49	2.84	0	0.003	0.037

The set of genes upregulated by NEK6 overexpression in castrate conditions correlated strongly with genes downregulated after castration in control tumors (Figure 4C), suggesting that NEK6 maintains gene expression lost with castration. The 60 overlapping genes in these two comparisons are listed in Supplemental Table S3A. The most statistically significant GO biological processes associated with the overlap (Supplemental Table S3B) are "cytokine-mediated signaling pathway" ($p=2\times10\text{-}5$) and "type I interferon signaling pathway" ($p=2\times10\text{-}5$), suggesting that maintenance of interferon and other immune-type signaling normally lost with castration may be involved in NEK6-mediated castration resistance.

Gene Expression changes mediated by NEK6 substrates

To determine the role of the identified substrates in mediating signaling downstream of NEK6, we assessed signaling in tumors mediated by phosphomimetic forms of these substrates with serine to aspartic acid substitutions of the phosphorylation sites identified *in vitro*, which we called FOXJ2(D×3) and NCOA5(D×3). We expressed them under a doxycycline-inducible promoter in tumors formed in male mice, which were harvested for RNA-Seq five days after castration from mice with continued doxycycline treatment or 7 day doxycycline withdrawal as for NEK6 previously. GSEA revealed that the gene expression changes mediated by a phosphomimetic form of FOXJ2 (FDR q-value=0.0044), but not NCOA5 (q=0.477) was statistically significantly correlated with the NEK6 signature (Figure 7A). Since NCOA5 failed to correlate to NEK6 signature, these observations suggest that the gene expression signatures associated with NEK6 and FOXJ2(D×3) expression are not the result of artifact or technical bias related to doxycycline treatment.

Eight genes overlapped between the gene expression signature mediated by FOXJ2(D×3) and NEK6 at the significance threshold used here (Figure 7B). Three of these eight genes, TPPP3 (Tubulin Polymerization-Promoting Protein Family Member 3), PSCA (Prostate Stem Cell Antigen), and PLAC8 (Placenta-Specific 8), had previously been found to be upregulated by NEK6 expression *in vitro* in the experiment described in Supplemental Figure S3D, suggesting these three genes as bona fide transcriptional targets of NEK6 signaling with FOXJ2 as the relevant transcription factor. Phosphorylation of FOXJ2 by NEK6 appears to increase stability of the FOXJ2 protein, as inducible expression of the phophomimetic form (D×3) leads to a significantly higher FOXJ2 protein expression as compared to wild-type and phosphorylation-deficient(A×3) forms (Figure 7C) despite similar mRNA levels (Figure 7D). This stabilized protein leads to increased expression of TPPP3 and PSCA *in vitro* (Figure 7D). TPPP3 has been previously implicated in proliferation, invasion and migration of cancer cells (Zhou *et al*., 2010), PSCA has been reported to promote growth and

metastasis of prostate cancer (Zhao, *et al*., 2015), and PLAC8 overexpression has been linked to EMT features and increased invasiveness (Li, *et al*., 2014), so these transcriptional targets may play a role in the oncogenic functions of NEK6.

Milestone 4: Phosphoproteomic studies reveal novel substrates FOXJ2, HUWE1, NCOA5, KRT18, TRA2B, HNRNPM, HNRNPA2B1, ZNF326. Gene expression studies reveal NEK6 likely mediates castration resistance through alteration of cell differentiation state and maintenance of immune-related signaling that is normally lost with castration. Phosphorylation of the NEK6 substrate FOXJ2 stabilizes the protein and increases transcription of downstream transcriptional targets TPPP3 and PSCA.

Milestone 5: Determine evidence for NEK6 and NLK conferring castrate resistance in clinical samples and identify subsets of patients displaying genomic changes and expression signatures corresponding to resistance mediated through the activity of a particular gene/pathway.

NEK6 is overexpressed in several malignant tissues and cell lines, and has been previously been implicated in cell transformation (Jeon *et al*., 2010; Nassirpour *et al*., 2010; Wang *et al*., 2014). Cancer types previously described to have high frequency of NEK6 overexpression include cancers of the liver (Chen *et al*., 2006; Jeon, *et al*., 2010; Cao, *et al*., 2012), stomach (Takeno, *et al*., 2008; Nassirpour *et al*., 2010), breast (Jeon *et al*., 2010; Nassirpour *et al*., 2010), uterus, colon/rectum and ovary (Nassirpour *et al*., 2010). In human prostate cancer, the NEK6 locus at chromosome 9q33.3 is present in a region of low level copy number gain (Taylor *et al*., 2010; Huang *et al*., 2012; Grasso *et al*., 2012) without a known validated prostate cancer oncogene. Genomic characterization of human prostate cancers through the Prostate TCGA and SU2C-PCF Dream Team efforts demonstrates amplification or mRNA overexpression (z-score>2) of NEK6 in 7% of primary tumors and 6% of metastases (www.cbioportal.org/prostate-portal/).

We performed immunohistochemistry analysis of primary prostate cancers compiled in seven tumor microarrays (TMA) generated by the Gelb Center for Translation Research at Dana-Farber Cancer Institute using an antibody we optimized for IHC (Supplemental Figure S2A and S2B). NEK6 expression was quantified by spectral imaging. We failed to find detectable levels of NEK6 protein in most prostate tissues, but found that NEK6 is aberrantly expressed in ~16% of tumors (Supplemental Figure S2C). NEK6 expression was greater in tumor samples than in benign-appearing glandular epithelium from these same radical prostatectomy specimens (one-tailed p=0.0012 by Student's T-test), suggesting that NEK6 expression is associated with tumor progression (Figure 2C).

It remains unclear at this point whether *de novo* acquisition of NEK6 amplification or overexpression is a mechanism of development of castration resistance in advanced prostate cancer. The strongest evidence for this would be detection of markers of overactive NEK6 signaling in metastatic CRPC in comparison to therapy-naïve samples, which per our model would be most likely to be detected in prostate cancers that have become AR-independent. A recent study by Grasso *et al* (2012) genetically profiled 35 cases of CRPC in comparison to 59 cases of localized PrCa. The primary difference in the genomic landscape in these two states was massive amplification of the AR in CRPC in comparison to the primary cases; there was no increase in amplitude of the region of copy number gain on 9q33.3 where NEK6 is located. There was no evidence for enrichment in genetic markers of any other signaling pathways in CRPC cases, though this is likely due to the fact that these cases were collected at a time when many of the current novel hormonal therapies had not yet been in widespread use. Efforts to genetically characterize larger numbers of CRPC cases, including those from patients who have progressed on novel hormonal therapies, are currently underway at DFCI (http://www.aacr.org/home/public--media/stand-up-to-cancer/su2c-dream-teams/su2c-pcf-dream-team-precision-therapy-of-advanced-prostate-cancer.aspx).

We analyzed the levels of NEK6 expression in several patient-derived prostate cell lines by immunoblotting (Figure 3A) and found that most prostate cancer cell lines expressed higher levels of NEK6 than immortalized (RWPE, PrEC-LH) and transformed (LHSR-AR) prostate epithelial cells. Interestingly, NEK6 levels were relatively high in VCaP and LNCaP cells, suggesting that high expression of NEK6 was not sufficient to overcome the *in vitro* androgen dependence of these cells; however, it is important to note that these cells were derived from patients with castration resistant disease *in vivo*. To test whether NEK6 was essential for *in vitro* proliferation of androgen-independent AR-low cell lines (reminiscent of the AR-low xenograft tumors), we introduced doxycycline-inducible shRNAs targeting NEK6 to CL-1, PC-3 and DU145 cells (Figure 3B). Despite near complete suppression of NEK6 expression, there was no effect on proliferation of the cell lines except a modest suppression of DU145 proliferation with shRNA#2 (Figure 3C). These

observations are in consonance with a prior report suggesting that NEK6 is not essential for proliferation of many mammalian cell lines (Nassirpour, *et al*., 2010).

Milestone 5: NEK6 is aberrantly expressed in a subset of primary human prostate cancer. Efforts to characterize metastatic biopsies from patients with CRPC for sequencing and assessing gene expression are underway.

Task 9: Genome wide screen of genes conferring androgen-independence to androgen-dependent cell line

Milestone 6: Identify a set of genes leading to androgen-independent prostate cancer cell growth in vitro and in vivo.

To ensure adequate representation of each gene in the kinome library in our original *in vivo* functional genomic screen, we implanted mice with LHSR-AR cells transduced with 9-10 ORF constructs in each pool. It would be impractical to expand this screen to a genome-wide library because of the number of mice and amount of material, time and effort required. In order to obtain a more manageable list of genes to query in our *in vivo* assay, we first aimed to identify genes that can confer androgen-independent proliferation to the androgen-dependent LNCaP prostate cancer cell line *in vitro*. This experiment was performed as a pooled screen using a barcoded lentivirally-delivered library encompassing ~20,000 ORFs available through the Broad Institute Genetic Perturbation Platform using the schema in Figure 8. The cells were infected at a target infection rate of 30% to achieve a multiplicity of infection (MOI) of 1 and target representation of 1000 cells infected with each ORF. The representation of ORFs at each time point were assessed by isolating genomic DNA, performing targeted sequencing of the barcodes, and deconvoluting enriched ORFs as represented by their corresponding barcodes. ORF representation was assessed at an early time point and after 7 weeks of selection, either in media with androgen-poor charcoal stripped serum (CSS) or media+CSS+2.5 uM enzalutamide, both compared with cells grown in androgen-containing media with fetal bovine serum (FBS) as a control. Three replicates were obtained for each condition.

There were >100 ORFs identified in the screen with a Z-score of >3 with regards to representation in the pool of cells harvested at the 7 week time point in the CSS+enzalutamide arm. These ORFs represent candidate genes conferring enzalutamide resistance to LNCaP cells. The top 48 ORFs are listed in Table 4 (genes listed twice reflect multiple ORFs representing the same gene).

Table 4. Genes sets enriched in ranked list of genes with decreased expression after castration (Control Day 5 vs. Day 2)

GENE	Z-SCORE	GENE	Z-SCORE	GENE	Z-SCORE
CREB5	14.53	MDM4	4.38	FGFR2	3.84
GRHL1	9.33	CDK6	4.32	GDAP2	3.75
PAX7	7.84	TRMT6	4.17	MTMR7	3.74
RARB	6.79	ATMIN	4.09	KLHL28	3.67
CDK4	5.76	C1QTNF9	4.07	GLRX3	3.63
MECP2	5.57	HNRNPCL1	4.07	RSPO3	3.56
FGF6	5.57	CDK4	4.04	SYN3	3.53
ALX1	5.48	OR1L3	4.02	CDK6	3.47
RARG	5.43	ZNF431	4.01	OR2A25	3.45
NTRK2	5.05	NR1I3	4.00	LMO1	3.45
INS	5.04	CDK4	3.93	NTRK2	3.44
ZNF16	5.01	ID1	3.93	PCCB	3.39
PHF23	4.73	CCND3	3.93	MAPK11	3.38
CDK6	4.60	VSX2	3.88	TBX15	3.38

CREB5 promotes tumorigenicity of PCa cells and ADT-resistance *in vivo*.

The top scoring gene in this screen was CREB5. CREB5 is a transcriptional factor overexpressed in colorectal cancers. To begin determining the role(s) of CREB5 in PCa, we overexpressed CREB5 or luciferase negative control in PCa cell lines including LAPC4, 22RV1, PC3, DU145 and C4-2, then cultured the cells in androgen-free media prior to exposure to CSS and enzalutamide. CREB5 rescued proliferation in the two androgen-sensitive lines (LnCAP, LAPC4),

and had a positive effect in 3 of the 4 insensitive lines (PC3, DU145, C4-2) (**Figure 10A**). To determine if CREB5 was necessary for proliferation, we next examined data from Project Achilles, in which we found that while all PCa lines (red dots) were relatively more CREB5 dependent than the normal prostate line (blue dot), the magnitude of relative dependency was modest compared to CDK4 suppression in the same PCa cells (**Figure 10B**). Overall, we concluded that CREB5 promotes ADT-resistance and has a small but consistent effect on PCa proliferation.

We next examined CREB5 regulation of tumor growth. mCRPC patients develop tumors even after ADT, thus these tumors grow in low androgen levels. After subcutaneously implanting xenografts of CREB5 or negative-control expressing LnCAP cells in castrated mice, tumors expressing CREB5 formed tumors more efficiently and grew larger (Fisher's exact, $p<0.005$) relative to luciferase control expressing cells 8 weeks post implant (**Figure 10C**). In a parallel experiment conducted in non-castrated mice, CREB5 also improved the overall grafting rate and average tumor size (students Fisher's exact, $p<0.005$) 5 weeks post implantation (**Figure 10C**), suggesting it also promotes general tumorigenicity. Enzalutamide is given to PCa patients with established advanced tumors, thus we next implanted xenografts of CREB5 or luciferase expressing cells, and allowed tumors to reach up to 250mm^3. At this point, to mimic the 2nd line of ADT, we castrated and treated mice with enzalutamide for over 4 weeks. In **Figure 3D**, CREB5 tumors were resistant to castration and continued to grow during the 4 weeks of enzalutamide treatment, while the overall volume of control tumors was conversely reduced by treatment. The MSKCC primary PCa cohort includes 10-year clinical outcomes matched to RNAseq data. In **Figure 10E**, patients with high CREB5 expression ($Z>2$) had high relapse rates (100%, 5/5) and lower median time to relapse (20.4 Months), and these were comparable to patients with high levels of AR ($Z>2$, 8/11. 18 Months) (**Figure 10E**). Overall, we demonstrate that CREB5 has strong association with PCa tumor growth.

KEY RESEARCH ACCOMPLISHMENTS

- Identification of NEK6 as a novel mediator of castration resistance in an *in vivo* forward functional genomic screen.
- Demonstration that kinase activity and continued expression of NEK6 is required for maintenance of castration resistance, suggesting its suitability as a therapeutic target.
- Discovery of novel NEK6 substrates FOXJ2, HUWE1, NCOA5, KRT18, TRA2B, HNRNPM, HNRNPA2B1, ZNF326 in cell culture.
- Determination that NEK6 overexpression in tumors leads to maintenance of immune-related signaling normally lost with castration, as well as squamous transdifferentiation
- Demonstration that phosphorylation of the NEK6 substrate FOXJ2 stabilizes the protein and increases transcription of downstream transcriptional targets TPPP3 and PSCA
- Determination that NEK6 is aberrantly expressed in a subset of human prostate cancer
- Identification of >100 candidates conferring enzalutamide resistance in a genome-wide barcoded ORF screen of genes conferring androgen independent proliferation of LNCaP cells *in vitro*
- Validation of CREB5 as a mediator of enzalutamide resistance *in vivo*

REPORTABLE OUTCOMES

Research Investigations

Adalsteinsson VA, Ha G, Freeman SS, Choudhury AD, Stover DG, Parsons H, Gydush G, Reed S, Loginov D, Livitz D, Rosebrock D, Leshchiner I, Kim J, Stewart C, Rosenberg M, Francis J, Zhang CZ, Cohen O, Oh C, Ding H, Lloyd M, Mahmud S, Helvie K, Merrill MS, Santiago RA, O'Connor E, Jeong SH, Leeson R, Barry R, Kramkowski J, Zhang Z, Polacek L, Lohr JG, Oliver N, Marini L, Harshman L, Tolaney S, Van Allen E, Winer EP, Lin NU, Nakabayashi M, Taplin ME, Johannessen CM, Garraway L, Golub TR, Boehm JS, Wagle N, Getz G, Love JC, Meyerson M. "Reproducible and scalable approach for whole-exome sequencing of cell-free DNA from patients with metastatic cancer." *Nature Communications.* Manuscript in press.

Choudhury AD, Schinzel AC, Cotter MB, Lis RT, Labella K, Lock YJ, Izzo F, Guney I, Bowden M, Li YY, Patel J, Hartman E, Carr SA, Schenone M, Jaffe JD, Kantoff PW, Hammerman PS, Hahn WC. "Castration resistance in prostate cancer is mediated by the kinase NEK6." Cancer Res. 2016 Nov 29. pii: canres.0455.2016.

Lohr JG, Adalsteinsson VA, Cibulskis K, Choudhury AD, Rosenberg M, Cruz-Gordillo P, Francis J, Zhang CZ, Shalek AK, Satija R, Trombetta JT, Lu D, Tallapragada N, Tahirova N, Kim S, Blumenstiel B, Sougnez C, Lowe A, Wong B, Auclair D, Van Allen EM, Nakabayashi M, Lis RT, Lee GM, Li T, Chabot MS, Ly A, Taplin ME, Clancy TE, Loda M, Regev A, Meyerson M, Hahn WC, Kantoff PW, Golub TR, Getz G, Boehm JS, Love JC. "Whole exome sequencing of CTCs as a window into metastatic prostate cancer." *Nat Biotechnol.* 2014 May;32(5):479-84.

Yao X, Choudhury AD, Yamanaka YJ, Adalsteinsson VA, Gierahn TM, Williamson CA, Lamb CR, Taplin ME, Nakabayashi M, Chabot MS, Li T, Lee GS, Boehm JS, Kantoff PW, Hahn WC, Wittrup KD, Love JC. "Functional analysis of single cells identifies a rare subset of circulating tumor cells with malignant traits." *Integr Biol (Camb).* 2014 Apr;6(4):388-98.

Reviews
Choudhury AD, Eeles R, Freedland SJ, Isaacs WB, Pomerantz MM, Schalken JA, Tammela TL, Visakorpi T. "The role of genetic markers in the management of prostate cancer." *Eur Urol.* 2012 Oct;62(4):577-87.

Choudhury AD, Kantoff PW. "New Agents in Metastatic Prostate Cancer". *J Natl Compr Canc Netw.* 2012 Nov 1;10(11):1403-9.

Abstracts, Poster Presentations and Exhibits Presented at Professional Meetings

Invited Presentations and Courses

Regional

2015 "NEK6 as a Novel Mediator of Castration Resistance in Prostate Cancer." RNAi/ MicroRNAs & Stem Cells (GeneExpression Systems), May 4, 2015, Cambridge MA.

2015 "Molecular Characterization of Circulating Tumor Cells in Prostate Cancer" ToPCaP Junior Investigators seminar. April 30, 2015, Boston MA.

2014 "Genetic Characterization and Analysis of CTCs in Clinical Practice." Circulate Symposium (Hanson Wade), November 20, 2014, Boston MA.

National

2016 "NEK6 mediates castration resistance in prostate cancer in vivo" Department of Defense PCRP Innovative Minds in Prostate Cancer Today (IMPaCT) Meeting. August 4, 2016. Towson, MD.

2014 "What, when and to whom? Controversies in systemic treatment of prostate cancer." Tatar Family Foundation Cancer Symposium. September 10, 2014, Dayton OH.

2013 "Functional and Genomic Characterization of Viable CTCs enabled by nanowells." 20th Annual Prostate Cancer Foundation Scientific Retreat. October 25, 2013. High achieving Young Investigator presentation.

2011 "Molecular Determinants of Hormone Refractory Prostate Cancer." 18th Annual Prostate Cancer Foundation Scientific Retreat, September 21, 2011, Young Investigator presentation.

Poster Presentations
Choudhury AD, Schinzel AC, Cotter MB, Lis RT, Labella K, Lock YJ, Izzo F, Guney I, Bowden M, Li YY, Patel J, Hartman E, Carr SA, Schenone M, Jaffe JD, Kantoff PW, Hammerman PS, Hahn WC. "NEK6

mediates castration resistance in prostate cancer in vivo" Department of Defense Innovative Minds in Prostate Cancer Today (IMPaCT) Meeting. August 4-5, 2016.

Choudhury AD, Lock J, Guney I, Pei T, Schinzel AC, Izzo F, Lis RT, Stack EC, Nakabayashi M, Werner L, Petrozziello G, Chabot M, Abelin J, Patel J, Jaffe JD, Kantoff PW, Loda M, Hahn WC. "An *in vivo* functional genomic screen identifies NEK6 as a novel mediator of castration resistance in prostate cancer." 7th Annual Multi-institutional Prostate Cancer Program Retreat, March 16-18, 2014. Poster selected for presentation.

Choudhury AD, Lohr JG, Adalsteinsson VA, Yao X, Cibulskis K, Rosenberg M, Sougnez C, Nakabayashi M, Lis RT, Lee GM, Li T, Chabot MS, Ly A, Taplin ME, Loda M, Kantoff PW, Golub TR, Wittrup KD, Getz G, Boehm JS, Love JC. "Functional and Genomic Characterization of Viable CTCs enabled by nanowells." Dana-Farber Cancer Institute Molecular and Cellular Oncology Department Retreat. January 27, 2014. 1st place winner.

Choudhury AD, Lohr JG, Adalsteinsson VA, Yao X, Cibulskis K, Rosenberg M, Sougnez C, Nakabayashi M, Lis RT, Lee GM, Li T, Chabot MS, Ly A, Taplin ME, Loda M, Kantoff PW, Golub TR, Wittrup KD, Getz G, Boehm JS, Love JC. "Functional and Genomic Characterization of Viable CTCs enabled by nanowells." Prostate Cancer Foundation 20th Annual Scientific Retreat. October 24-26, 2013.

Choudhury AD, Guney I, Schinzel AC, Izzo F, Stack EC, Nakabayashi M, Petrozziello G, Hahn WC. "Molecular Determinants of Hormone Refractory Prostate Cancer." 5th Annual Multi-institutional Prostate Cancer Program Retreat, March 19-21, 2012. Poster selected for presentation and awarded as a prize winner.

Choudhury AD, Guney I, Schinzel AC, Izzo F, Stack EC, Nakabayashi M, Petrozziello G, Hahn WC. "Molecular Determinants of Hormone Refractory Prostate Cancer." Dana-Farber Cancer Institute Molecular and Cellular Oncology Department Retreat. April 9, 2012.

CONCLUSIONS

We have performed an unbiased *in vivo* functional genomic screen to identify kinases that can confer androgen independence in a model of androgen-dependent prostate tumor formation, and discovered NEK6 as a novel mediator of castration resistance. The NEK6 gene on 9q33.3 is located on a region of recurrent copy number gain in prostate cancer, and it is overexpressed in a subset of primary human prostate cancers and most patient-derived prostate cancer cell lines tested. We are unable to correlate protein expression to amplification of the locus or mRNA overexpression in these samples, so it is unknown whether aberrant NEK6 protein expression is driven by genetic/transcriptional changes vs. other translational or post-translational determinants of protein levels. NEK6 plays a mechanistic role in the development of castration resistance in our model, and turning off its expression in xenograft tumors where it is overexpressed restores sensitivity to castration, suggesting that its continued activity is required for tumor maintenance in this context. The finding that NEK6 is not essential for mammalian cells, along with the fact that mice homozygous for a targeted null NEK6 allele (**Nek6^{tm1Dgen}**) demonstrate no apparent phenotype (https://www.infrafrontier.eu/sites/infrafrontier.eu/files/upload/public/deltagen/DELTAGEN_T518/) except for promotion of cardiac hypertrophy induced by transthoracic aorta constriction (Bian *et al*., 2014), suggests that NEK6 could be safely therapeutically targeted in prostate cancer and other cancer types where it is a relevant driver without a high degree of systemic toxicity.

The role of NEK6 in oncogenic signaling have been proposed to be mediated by cell cycle progression/cyclin B modulation (Zhang *et al*., 2014), inhibition of p53-mediated senescence (Jee *et al*., 2010), phosphorylation of STAT3 (Jeon *et al*., 2010), and blocking nuclear translocation of SMAD4 to antagonize TGFβ signaling (Zuo *et al*., 2014). Here we failed to find evidence to implicate any of these previously described mechanisms in the role of NEK6-mediated castration resistance. Specifically, we did not find gene sets annotated as involving STAT3, Wnt/β-catenin or TGFβ/SMAD4 signaling within the top 200 gene sets correlated with the NEK6 signature by GSEA in tumors after castration; rather, cytoskeletal, differentiation, and immune processes are implicated. In particular, NEK6 overexpression maintains the expression of a set of genes involved in interferon signaling that is normally lost with castration in this model. Relevance of interferon-related gene sets in prostate cancer has been demonstrated previously in signaling differences between cancers in patients with African and European ancestry (Wallace *et al*., 2008) and in treatment resistance (Cheon *et al*., 2013). Recent reports also implicated immune signaling (Bishop *et al*., 2015) and cytoskeletal signaling (by induction of RhoA ,Cdc42, and Rac1) (Miyamoto *et al*., 2015) as mechanisms of resistance to the anti-

androgen enzalutamide. Here, analysis of gene expression changes induced by a phosphomimetic form of a newly identified substrate FOXJ2 revealed that this is the relevant transcription factor for certain important transcriptional targets downstream of NEK6 and thus demonstrates a novel role for this pathway in castration-resistant tumor formation.

Parallel growth factor signaling has been implicated in androgen independence in several model systems, but this phenotype depends on both the growth factor milieu of the microenvironment and the underlying genetic context of the cancer cells with regards to their behavior in this milieu. The use of engineered cell lines allows control over the genetic context, and the use of xenografts allows testing different *in vivo* environments where the limiting nutrients and growth factors are unknown and thus could not be replicated in a culture environment. While NEK6 is a potent mediator of castration resistance in this model, it is reasonable to consider that other genes might be identified to confer androgen independence in different genetic contexts in different microenvironments.

As such, we performed a genome-wide ORF screen to identify mediators of resistance to androgen deprivation and enzalutamide in LNCaP cells in vitro. We identified >100 genes conferring this phenotype, with the top candidate being the transcription factor CREB5. We found that CREB5 enhanced the tumorigenicity of prostate cancer xenografts in vivo and conferred enzalutamide resistance to xenografts.

While alterations in the AR gene and in AR-mediated signaling have already been demonstrated to play a role in the development of castration resistance (Sharifi, 2013), it is apparent that resistance to hormonal therapies can arise through progression to states where the androgen receptor is no longer essential for survival, collectively termed androgen pathway independent prostate cancer (APIPC) (Nelson, 2012). A subset of these cancers express markers of neuroendocrine differentiation, and transdifferentiation to a squamous phenotype has also been described in resistance to hormonal therapy (Humphrey, 2012); however, the molecular mechanisms underlying transition to APIPC are not fully characterized. Specifically, we hypothesize that APIPC represents a diversity of phenotypes and dependencies; a comprehensive understanding of these mechanisms would identify potential therapeutic targets for intervention, and would also allow for biomarker discovery to stratify patients for likelihood of response to targeted therapies (Choudhury, Eeles, *et al*., 2012). Thus, the signaling pathways described here warrant further study in this patient population.

REFERENCES

Abrahamsson PA. Neuroendocrine differentiation in prostatic carcinoma. Prostate. 1999 May;39(2):135-48.

Araujo JC, Trudel GC, Saad F, *et al*. Docetaxel and dasatinib or placebo in men with metastatic castration-resistant prostate cancer (READY): a randomised, double-blind phase 3 trial. Lancet Oncol. 2013 Dec;14(13):1307-16.

Attard G, Reid AH, A'Hern R, Parker C, Oommen NB, Folkerd E, Messiou C, Molife LR, Maier G, Thompson E, Olmos D, Sinha R, Lee G, Dowsett M, *et al.* (2009) Selective inhibition of CYP17 with abiraterone acetate is highly active in the treatment of castration-resistant prostate cancer. J Clin Oncol. 2009 Aug 10;27(23):3742-8. http://jco.ascopubs.org/content/27/23/3742.long

Belham C, Comb MJ, Avruch J. Identification of the NIMA family kinases NEK6/7 as regulators of the p70 ribosomal S6 kinase. Curr Biol. 2001 Aug 7;11(15):1155-67.

Belham C, Roig J, Caldwell JA, *et al*. A mitotic cascade of NIMA family kinases. Nercc1/Nek9 activates the Nek6 and Nek7 kinases. J Biol Chem. 2003 Sep 12;278(37):34897-909.

Berger, R., Febbo, P.G., Majumder, P.K., Zhao, J.J., Mukherjee, S., Signoretti, S., *et al.* (2004). Androgen-induced differentiation and tumorigenicity of human prostate epithelial cells. Cancer Res *64*, 8867-8875. http://cancerres.aacrjournals.org/content/64/24/8867.long

Bian Z, Liao H, Zhang Y, *et al*. Never in mitosis gene A related kinase-6 attenuates pressure overload-induced activation of the protein kinase B pathway and cardiac hypertrophy. PLoS One. 2014 Apr 24;9(4):e96095.

Bishop JL, Sio A, Angeles A, Roberts ME, Azad AA, Chi KN, *et al*. PD-L1 is highly expressed in Enzalutamide resistant prostate cancer. Oncotarget 2015;6(1):234-42.

Bosco A, Ehteshami S, Stern DA, Martinez FD. Decreased activation of inflammatory networks during acute asthma exacerbations is associated with chronic airflow obstruction. Mucosal Immunol. 2010 Jul;3(4):399-409. doi: 10.1038/mi.2010.13. Epub 2010 Mar 24.

Cao X, Xia Y, Yang J, *et al*., Clinical and biological significance of never in mitosis gene A-related kinase 6 (NEK6) expression in hepatic cell cancer. Pathol Oncol Res. 2012 Apr;18(2):201-7.

Carver BS, Chapinski C, Wongvipat J, *et al*. Reciprocal feedback regulation of PI3K and androgen receptor signaling in PTEN-deficient prostate cancer. Cancer Cell. 2011 May 17;19(5):575-86.

Chen J, Li L, Zhang Y, *et al*. Interaction of Pin1 with Nek6 and characterization of their expression correlation in Chinese hepatocellular carcinoma patients. Biochem Biophys Res Commun. 2006 Mar 24;341(4):1059-65.

Cheon H, Holvey-Bates EG, Schoggins JW, *et al*. IFNβ-dependent increases in STAT1, STAT2, and IRF9 mediate resistance to viruses and DNA damage. EMBO J. 2013 Oct 16;32(20):2751-63.

Choudhury AD, Eeles R, Freedland SJ, *et al*. The role of genetic markers in the management of prostate cancer. Eur Urol. 2012 Oct;62(4):577-87.

Choudhury AD, Kantoff PW. New agents in metastatic prostate cancer. J Natl Compr Canc Netw. 2012 Nov 1;10(11):1403-9.

Cruciat CM. Casein kinase 1 and Wnt/β-catenin signaling. Curr Opin Cell Biol. 2014 Dec;31:46-55. doi: 10.1016/j.ceb.2014.08.003. Epub 2014 Sep 15.

Dirmeier U, Hoffmann R, Kilger E, *et al*. Latent membrane protein 1 of Epstein-Barr virus coordinately regulates proliferation with control of apoptosis. Oncogene. 2005 Mar 3;24(10):1711-7.

Edwards, J., and Bartlett, J.M. (2005a). The androgen receptor and signal-transduction pathways in hormone-refractory prostate cancer. Part 1: Modifications to the androgen receptor. BJU Int *95*, 1320-1326.

Edwards J, Bartlett JM. (2005b) The androgen receptor and signal-transduction pathways in hormone-refractory prostate cancer. Part 2: Androgen-receptor cofactors and bypass pathways. BJU Int. 2005 Jun;95(9):1327-35.

Drake JM, Graham NA, Stoyanova T, *et al*. Oncogene-specific activation of tyrosine kinase networks during prostate cancer progression. Proc Natl Acad Sci U S A. 2012 Jan 31;109(5):1643-8.

Drake JM, Graham NA, Lee JK, *et al.* Metastatic castration-resistant prostate cancer reveals intrapatient similarity and interpatient heterogeneity of therapeutic kinase targets. Proc Natl Acad Sci U S A. 2013 Dec 3;110(49):E4762-9.

Grasso CS, Wu YM, Robinson DR, *et al*. The mutational landscape of lethal castration-resistant prostate cancer. Nature. 2012 Jul 12;487(7406):239-43.

Guo Z, Dai B, Jiang T, Xu K, Xie Y, Kim O, Nesheiwat I, Kong X, Melamed J, Handratta VD, *et al.* (2006) Regulation of androgen receptor activity by tyrosine phosphorylation. Cancer Cell. 2006 Oct;10(4):309-19. http://www.sciencedirect.com/science/article/pii/S1535610806002777

Hieronymus H, Lamb J, Ross KN, *et al*. Gene expression signature-based chemical genomic prediction identifies a novel class of HSP90 pathway modulators. Cancer Cell. 2006 Oct;10(4):321-30.

Hu Y, Song W, Cirstea D, Lu D, Munshi NC, Anderson KC. CSNK1α1 mediates malignant plasma cell survival.Leukemia. 2015 Feb;29(2):474-82.

Huang S, Gulzar ZG, Salari K, Lapointe J, Brooks JD, Pollack JR. Recurrent deletion of CHD1 in prostate cancer with relevance to cell invasiveness. Oncogene. 2012 Sep 13;31(37):4164-70.

Humphrey PA. Histological variants of prostatic carcinoma and their significance. Histopathology. 2012 Jan;60(1):59-74.

Järås M, Miller PG, Chu LP, *et al*. Csnk1a1 inhibition has p53-dependent therapeutic efficacy in acute myeloid leukemia. J Exp Med. 2014 Apr 7;211(4):605-12.

Jee HJ, Kim AJ, Song N, *et al*. Nek6 overexpression antagonizes p53-induced senescence in human cancer cells. Cell Cycle. 2010 Dec 1;9(23):4703-10.

Jeon YJ, Lee KY, Cho YY, Pugliese A, Kim HG, Jeong CH, *et al.* (2010) Role of NEK6 in tumor promoter-induced transformation in JB6 C141 mouse skin epidermal cells. J Biol Chem. 2010 Sep 3;285(36):28126-33. http://www.jbc.org/content/285/36/28126.long

Lam JS, Yamashiro J, Shintaku IP, *et al*. (2005). "Prostate stem cell antigen is overexpressed in prostate cancer metastases.". Clin. Cancer Res. 11 (7): 2591–6.

Li C, Ma H, Wang Y, Cao Z, Graves-Deal R, Powell AE, *et al*. Excess PLAC8 promotes an unconventional ERK2-dependent EMT in colon cancer. The Journal of clinical investigation 2014;124(5):2172-87.

Lin, H.K., Yeh, S., Kang, H.Y., and Chang, C. (2001). Akt suppresses androgen-induced apoptosis by phosphorylating and inhibiting androgen receptor. Proc Natl Acad Sci U S A *98*, 7200-7205. http://www.pnas.org/content/98/13/7200.long

Liu Y, Mo JQ, Hu Q, Boivin G, Levin L, Lu S, *et al*. Targeted overexpression of vav3 oncogene in prostatic epithelium induces nonbacterial prostatitis and prostate cancer. Cancer research 2008;68(15):6396-406.

Lizcano JM, Deak M, Morrice N, *et al*. Molecular basis for the substrate specificity of NIMA-related kinase-6 (NEK6). Evidence that NEK6 does not phosphorylate the hydrophobic motif of ribosomal S6 protein kinase and serum- and glucocorticoid-induced protein kinase *in vivo*. J Biol Chem. 2002 Aug 2;277(31):27839-49.

Matsuda A, Suzuki Y, Honda G, *et al*. Large-scale identification and characterization of human genes that activate NF-kappaB and MAPK signaling pathways. Oncogene. 2003 May 22;22(21):3307-18.

Mendiratta P, *et al*. Genomic strategy for targeting therapy in castration-resistant prostate cancer. *J Clin Oncol.* 2009 Apr 20;27(12):2022-9.

Miyamoto DT, Zheng Y, Wittner BS, Lee RJ, Zhu H, Broderick KT, *et al*. RNA-Seq of single prostate CTCs implicates noncanonical Wnt signaling in antiandrogen resistance. Science 2015;349(6254):1351-6.

Mulholland DJ, Tran LM, Li Y, *et al*. Cell autonomous role of PTEN in regulating castration-resistant prostate cancer growth. Cancer Cell. 2011 Jun 14;19(6):792-804.

Nassirpour R, Shao L, Flanagan P, *et al*. Nek6 mediates human cancer cell transformation and is a potential cancer therapeutic target. Mol Cancer Res. 2010 May;8(5):717-28.

Nelson PS. Molecular states underlying androgen receptor activation: a framework for therapeutics targeting androgen signaling in prostate cancer. J Clin Oncol. 2012 Feb 20;30(6):644-6.

O'Regan L, Fry AM. The Nek6 and Nek7 protein kinases are required for robust mitotic spindle formation and cytokinesis. Mol Cell Biol. 2009 Jul;29(14):3975-90.

Palanisamy N, Ateeq B, Kalyana-Sundaram S, Pflueger D, Ramnarayanan K, *et al.* (2010) Rearrangements of the RAF kinase pathway in prostate cancer, gastric cancer and melanoma. Nat Med. 2010 Jul;16(7):793-8. http://www.nature.com/nm/journal/v16/n7/full/nm.2166.html

Pienta, K.J., and Bradley, D. (2006). Mechanisms underlying the development of androgen-independent prostate cancer. Clin Cancer Res *12*, 1665-1671. http://clincancerres.aacrjournals.org/content/12/6/1665.long

Qin J, Lee HJ, Wu SP, Lin SC, Lanz RB, Creighton CJ, DeMayo FJ, Tsai SY, Tsai MJ. Androgen deprivation-induced NCoA2 promotes metastatic and castration-resistant prostate cancer. J Clin Invest. 2014 Nov;124(11):5013-26.

Ren K, Gou X, Xiao M, *et al*. The over-expression of Pim-2 promote the tumorigenesis of prostatic carcinoma through phosphorylating eIF4B. Prostate. 2013 Sep;73(13):1462-9.

Richards MW, O'Regan L, Mas-Droux C, *et al*. An autoinhibitory tyrosine motif in the cell-cycle-regulated Nek7 kinase is released through binding of Nek9. Mol Cell. 2009 Nov 25;36(4):560-70.

Scher HI, Fizazi K, Saad F, Taplin ME, *et al*; AFFIRM Investigators. Increased survival with enzalutamide in prostate cancer after chemotherapy. N Engl J Med. 2012 Sep 27;367(13):1187-97.

Schneider RK, Ademà V, Heckl D, *et al*. Role of casein kinase 1A1 in the biology and targeted therapy of del(5q) MDS. Cancer Cell. 2014 Oct 13;26(4):509-20.

Sequist LV, Waltman BA, Dias-Santagata D, *et al*. Genotypic and histological evolution of lung cancers acquiring resistance to EGFR inhibitors. Sci Transl Med. 2011 Mar 23;3(75):75ra26.

Sharifi N. Mechanisms of androgen receptor activation in castration-resistant prostate cancer. Endocrinology. 2013 Nov;154(11):4010-7.

Sharma NL, Massie CE, Ramos-Montoya A, *et al.* The androgen receptor induces a distinct transcriptional program in castration-resistant prostate cancer in man. Cancer Cell. 2013 Jan 14;23(1):35-47.

Smith MR, Sweeney CJ, Corn PG, *et al*. Cabozantinib in chemotherapy-pretreated metastatic castration-resistant prostate cancer: results of a phase II nonrandomized expansion study. J Clin Oncol. 2014 Oct 20;32(30):3391-9.

Stoyanova T, Cooper AR, Drake JM, *et al*. Prostate cancer originating in basal cells progresses to adenocarcinoma propagated by luminal-like cells. Proc Natl Acad Sci U S A. 2013 Dec 10;110(50):20111-6.

Subramanian A, Tamayo P, *et al.* (2005) Gene set enrichment analysis: a knowledge-based approach for interpreting genome-wide expression profiles. Proc Natl Acad Sci U S A. 2005 Oct 25;102(43):15545-50. http://www.pnas.org/content/102/43/15545.long

Sun, H., Fang, H., Chen, T., Perkings, R., and Tong, W., "GOFFA: Gene Ontology For Functional Analysis - Software for gene ontology-based functional analysis of genomic and proteomic data." BMC Bioinformatics, 7(Suppl 2):S23, 2006.

Takeno A, Takemasa I, Doki Y, *et al*. Integrative approach for differentially overexpressed genes in gastric cancer by combining large-scale gene expression profiling and network analysis. Br J Cancer. 2008 Oct 21;99(8):1307-15.

Tao S, He H, Chen Q. ChIP-seq analysis of androgen receptor in LNCaP cell line. Mol Biol Rep. 2014 Sep;41(9):6291-6.

Taylor BS, Schultz N, Hieronymus H, Gopalan A, Xiao Y, Carver BS, Arora VK, Kaushik P, Cerami E, Reva B, *et al.* (2010) Integrative genomic profiling of human prostate cancer. Cancer Cell. 2010 Jul 13;18(1):11-22. http://www.sciencedirect.com/science/article/pii/S1535610810002382

Tran CP, Lin C, Yamashiro J, Reiter RE (2003). Prostate stem cell antigen is a marker of late intermediate prostate epithelial cells. Mol. Cancer Res. 1 (2): 113–21.

Tran, C., Ouk, S., Clegg, N.J., Chen, Y., Watson, P.A., Arora, V., Wongvipat, J., *et al.* (2009). Development of a second-generation antiandrogen for treatment of advanced prostate cancer. Science *324*, 787-790.http://www.sciencemag.org/content/324/5928/787.full

van Dorst EB, van Muijen GN, Litvinov SV, Fleuren GJ. The limited difference between keratin patterns of squamous cell carcinomas and adenocarcinomas is explicable by both cell lineage and state of differentiation of tumour cells. J Clin Pathol. 1998 Sep;51(9):679-84.

Vaz Meirelles G, Ferreira Lanza DC, da Silva JC, Santana Bernachi J, Paes Leme AF, Kobarg J. Characterization of hNek6 interactome reveals an important role for its short N-terminal domain and colocalization with proteins at the centrosome. J Proteome Res. 2010 Dec 3;9(12):6298-316.

Wallace TA, Prueitt RL, Yi M, *et al*. Tumor immunobiological differences in prostate cancer between African-American and European-American men. Cancer Res. 2008 Feb 1;68(3):927-36.

Wang Y, Lee YM, Baitsch L, *et al*. MELK is an oncogenic kinase essential for mitotic progression in basal-like breast cancer cells. Elife. 2014 May 20;3:e01763.

Weichselbaum RR, Ishwaran H, Yoon T, *et al*. An interferon-related gene signature for DNA damage resistance is a predictive marker for chemotherapy and radiation for breast cancer. Proc Natl Acad Sci U S A. 2008 Nov 25;105(47):18490-5.

Whang YE, Armstrong AJ, Rathmell WK, Godley PA, Kim WY, Pruthi RS, Wallen EM, Crane JM, Moore DT, Grigson G, Morris K, Watkins CP, George DJ. (2011) A phase II study of lapatinib, a dual EGFR and HER-2 tyrosine kinase inhibitor, in patients with castration-resistant prostate cancer. Urol Oncol. 2011 Mar 9.

Yeh, S., Lin, H.K., Kang, H.Y., Thin, T.H., Lin, M.F., and Chang, C. (1999). From HER2/Neu signal cascade to androgen receptor and its coactivators: a novel pathway by induction of androgen target genes through MAP kinase in prostate cancer cells. Proc Natl Acad Sci U S A *96*, 5458-5463. http://www.pnas.org/content/96/10/5458.long

Yin MJ, Shao L, Voehringer D, Smeal T, Jallal B. The serine/threonine kinase Nek6 is required for cell cycle progression through mitosis. J Biol Chem. 2003 Dec 26;278(52):52454-60.

Yokoyama NN, Shao S, Hoang BH, Mercola D, Zi X. Wnt signaling in castration-resistant prostate cancer: implications for therapy. Am J Clin Exp Urol. 2014 Apr 15;2(1):27-44.

Zhang B, Zhang H, Wang D, *et al*. Never in mitosis gene A-related kinase 6 promotes cell proliferation of hepatocellular carcinoma via cyclin B modulation. Oncol Lett. 2014 Sep;8(3):1163-1168.

Zhao Z, He J, Kang R, Zhao S, Liu L, Li F. RNA interference targeting PSCA suppresses primary tumor growth and metastasis formation of human prostate cancer xenografts in SCID mice. The Prostate 2015.

Zhou W, Li J, Wang X, Hu R. Stable knockdown of TPPP3 by RNA interference in Lewis lung carcinoma cell inhibits tumor growth and metastasis. Molecular and cellular biochemistry 2010;343(1-2):231-8.

Zuo J, Ma H, Cai H, Wu Y, Jiang W, Yu L. An inhibitory role of NEK6 in TGFβ/Smad signaling pathway. BMB Rep. 2014 Dec 18.

Medical and Cellular Oncology retreat, and this work has resulted in two publications to this point. I have since been awarded two grants to study circulating tumor cells in comparison to extensively sampled matched metastatic tissue in patients undergoing rapid autopsy, and in patients participating in a clinical trial of a combination of crizotinib and enzalutamide. These projects have now expanded into studying circulating free DNA from patients with metastatic prostate cancer – we have demonstrated a workflow for performing high quality whole exome sequencing from both fresh and banked plasma, and a manuscript describing this process has been preliminarily accepted to *Nature Communications*. We are currently testing this workflow as a way to monitor tumor burden and subclonal changes over time in patients being treated on study, and are planning large scale projects to assess for predictors of response and resistance to carboplatin and docetaxel chemotherapy from banked plasma.

My training program at Dana Farber Cancer Institute and my involvement with the Broad Institute of MIT and Harvard has me uniquely positioned to apply novel experimental approaches to address rapidly evolving clinical problems in prostate cancer. This experience has led to my selection as the PI of the correlative studies associated with a planned Alliance trial of docetaxel and radium-223 in hormone sensitive prostate cancer. In addition, I am the site PI of a rapid autopsy protocol developed with Dr. Glenn Bubley from BIDMC. For institutional service, I have worked with Dr. Aymen Elfiky for the development and implementation of clinical pathways into the genitourinary oncology department, lead the case discussions at the GU Tumor Board, and serve on the Scientific Review Committee 1.

In my independent academic faculty position, I plan to pursue cutting edge translational research in genitourinary malignancies. I hope to molecularly characterize patient tissue to assess for markers of disease progression and resistance, and design investigator-initiated clinical trials for the study of novel therapeutics and to acquire further tissue for study. With my background in molecular biology and genomics, along with my clinical training and experience in collaborative translational studies, I believe I am well positioned to achieve my career goals given the environment and opportunity.

SUPPORTING DATA

Figure 1. NEK6 confers androgen-independent tumor formation in a xenograft model of androgen-dependent prostate cancer. A. Tumor formation at 60 d for parental LHSR-AR cells and cells expressing NEK6 in female and castrated mice. B. Tumor formation at 60 d for parental LHMK-AR cells and cells expressing NEK6 in female mice. C. Left: Inducible expression of NEK6 *in vitro* at 48 hrs after addition of doxycycline Right: Waterfall plot of change in tumor volume at 30 d after castration (compared to prior to castration) of xenograft tumors derived from parental LHSR-AR cells and cells with inducible NEK6 expression formed in male mice.

Figure 2. A. NEK6-mediated androgen-independent tumors are primarily squamous in histology and AR negative. Sections of tumors derived from parental LHSR-AR cells expressing GFP in male mice, and cells expressing NEK6 in female and castrated mice were stained with AR antibody (brown). B. Sections of tumors derived from LHSR-AR cells overexpressing NEK6 in male mice with implanted testosterone pellet harvested prior to castration (Day 0) and at 4, 8, and 12 d after castration. C. Immunohistochemical staining at 20x magnification for NEK6 in prostate cancer tissue microarrays. Low (left and middle) and high grade (right) cases are represented, each core showing tumor infiltrating in between benign glands with higher expression seen in the tumor.

Figure 3. NEK6 is overexpressed in several prostate cancer cell lines compared to immortalized (RWPE, LH) and transformed (LHSR-AR) prostate epithelial cells. A. Left: Expression of NEK6 and AR in prostate cell lines with Hsp90 as loading control; Right: NEK6 expression in LHSR-AR cells overexpressing NEK6 (column 2), and in VCaP and LNCaP cells. B. Expression of NEK6 in CL-1, PC-3, and DU145 cells with doxycycline inducible expression of 2 shRNAs targeting NEK6 or a control targeting lacZ in the presence or absence of doxycycline (CL-1 and PC-3) or with doxycycline in the presence or absence of growth factor stimulation (DU145). C. Proliferation curves of cells cultured in the presence of doxycycline with cells in 60 mm plates, split and replated every 2-3 d as indicated. The average of 3 replicates with error bars is shown.

Figure 4. A. Immunoblots of protein lysates of xenograft tumors derived from LHSR-AR cells transduced with doxycycline-inducible constructs (in the pTRIPz vector) for the expression of GFP or NEK6 in male mice, with doxycycline maintained in the diet at time of harvest (+dox) or with doxycycline diet removed 7 d prior to harvest (-dox). Tumors were harvested from non-castrated mice (day 0) or 2 or 5 d after castration. Short and long exposures of the NEK6 immunoblot are shown. B. Gene Set Enrichment Analysis performed on the gene expression signature mediated by NEK6 overexpression at d 5 after castration (GSEA pre-ranked based on ratio of classes to tumors without NEK6 overexpression). The top two curated gene sets (C2) from the molecular signatures database (MSigDB) correlated with the NEK6 signature are shown. C. Left: Genes downregulated in the control (-dox) tumors after castration (fold change <-1.5, signal-to-noise <-1 in the comparison of tumors harvested at d 5 and day 2) were plotted against the NEK6 signature at d 5 using GSEA pre-ranked. Right: Venn diagram of genes downregulated in control tumors after castration intersected with genes upregulated by NEK6 at day 5 (fold change >1.5, signal-to-noise >1 in the comparison of +dox to -dox tumors). The GO terms most highly enriched in this overlap are cytokine-mediated and type I interferon signaling pathways (p=2x10-5).

Figure 5. A. 293T cells were transfected with expression constructs for the indicated kinases with a C-terminal V5 tag and immune complexes isolated with an anti-V5 antibody. Eluates from 1/4 of the beads were assayed by V5 immunoblot; the remaining 3/4 was subjected to on-bead *in vitro* kinase assay with recombinant active GST-NEK6 (Sigma). B+C. Kinase assay performed as in (A) but with wild-type or mutant forms of CSNK1A1 or YES1 as indicated: + indicates a mutation is present at that residue, - indicates that the residue is wild-type (lane 1 of each blot represents the wild-type protein). 5% of the input assayed by V5 immunoblot is shown in the left panels; the kinase assay is shown in the right panels.

Figure 6. A. NEK6 can phosphorylate NCOA5 and FOXJ2 *in vitro* at the sites discovered in the phosphoproteomic screen. 293T cells were transfected with expression constructs for wild-type and mutant (S-to-D) versions of NCOA5 or FOXJ2 with a C-terminal V5 tag and immunoprecipitated with anti-V5 antibody. Eluates from 1/5 of the beads were assayed by V5 immunoblot; the remaining 4/5 was subjected to on-bead *in vitro* kinase assay with recombinant active GST-NEK6 (Sigma). B+C. Kinase assay performed as in (A) but with wild-type or mutant forms of FOXJ2 or NCOA5 as indicated: + indicates a mutation is present at that residue, - indicates that the residue is wild-type (lane 1 of each blot represents the wild-type protein). 5% of the input assayed by V5 immunoblot is shown in the left panels; the kinase assay is shown in the right panels. FOXJ2 has 10 S/T residues of the previously reported NEK6 motif L/F/W/Y-X-X-pS/pT-F/W/Y/M/L/I/V/R/K; the six residues in FOXJ2 (or homologous residues in FOXJ3) that had been previously demonstrated to be phosphorylated in phosphosite.org were assayed here. NCOA5 has 5 S/T residues in this NEK6

phosphorylation motif; however, mutating Ser201 to aspartic acid dramatically decreased exogenous NCOA5 expression, so the remaining four sites were tested in this assay.

Figure 7. A. RNA-Seq was performed from 3 tumors inducibly expressing phosphomimetic forms of FOXJ2 or NCOA5 with continued doxycycline expression, and 3 matched tumors seven days post doxycycline withdrawal, 5 days after castration. Shown are plots demonstrating correlation of genes upregulated by these phosphomimetic forms with the NEK6 signature at day 5 by GSEA pre-ranked. B Overlap of genes upregulated by NEK6 and by FOXJ2(D×3)C. Immunoblot of protein lysates of LHSR-AR cells transduced with doxycycline-inducible constructs (in the pTRIPz vector) for the expression of phosphorylation-deficient (A×3), wild-type, and phosphomimetic (D×3) forms of FOXJ2 treated with or without doxycycline for 48 hours. D. Gene expression of FOXJ2, TPPP3 and PSCA by quantitative RT-PCR (as fold-change from control) in cells expressing (A×3), wild-type and (D×3) forms of FOXJ2 under a doxycycline-inducible promoter treated with or without doxycycline for 48 hours. The average of 3 technical replicates (with error bars representing the standard deviation) is shown.

Figure 8. Schema for *in vitro* genome-wide ORF screen in LNCaP cells grown in fetal bovine serum (FBS), charcoal-stripped serum (CSS), and charcoal-stripped serum with enzalutamide (CSS+ENZA).

Figure 9. Distribution of Z-scores (y-axis) representing the relative representation as compared to the mean of all of the ORFs represented (x-axis) in the CSS+ENZA arm of the screen. Red lines denote our statistical threshold of Z-score >+3 for ORFs increasing proliferation under these conditions, and Z-score <3 for ORFs sensitizing cells to these conditions.

Figure 10. A. The relative proliferation of PCa cell lines overexpressing CREB5 or luciferase control are shown. In immuno-blots performed of the cell lysates, V5 indicates expression of epitope-tagged CREB5 or luciferase. Tubulin is used as a loading control. B. Of the Project Achilles database, the relative dependency of CREB5 (top) and CDK4 (bottom) are shown across all assayed 503 cell lines. All PCa lines (red) are more sensitive compared to the normal epithelial prostate line (blue) to RNAi; however, the y-axis scale indicates that CDK4 suppression had a greater effect. C. Xenografts of CREB5 or luciferase expressing LnCAP cells were implanted in the flanks or either castrated (left, 8 weeks) or healthy (right, 5 weeks) immuno-deficient BALB/C mice. At the experimental end point, tumor volumes were measured and plotted ($p<0.005$, Fisher's exact). D. CREB5 or luciferase expressing xenografts are implanted, and after forming tumors, the mice are castrated and treated with enzalutamide for 4 weeks. Left, the average growth rate of CREB5 (red) or luciferase (black) xenografts are shown relative to time (days). Right, the overall response for individual tumors is shown. E. Of the MSKCC PCa cohort, the relapse rate is plotted for PCa tumors expressing high levels of CREB5 (red, Z>2) or AR (blue, Z>2) relative to all other tumors (green). The table summarizes relapsed patients, median time and p-value.

Supplemental Figure S1. A. Tumor formation at 60 d for LHSR-AR cells expressing wild-type and kinase-dead NEK6 in castrated mice. B. Tumor formation at 60 d for LHSR-AR cells expressing NEK6 as well as a doxycycline-inducible short-hairpin RNA targeting the androgen receptor (AR) in female mice with or without doxycycline in their diet.

Supplemental Figure S2. A. Immunoblots using Epitomics 3789-1 (left) and Santa Cruz H-50 (right) anti-NEK6 primary antibodies on protein lysates of LHSR-AR cells transduced with a doxycycline-inducible construct for the expression of NEK6 with (+) or without (-) the addition of doxycycline in the media for 48 hrs. B. Immunohistochemistry of xenograft tumors derived from LHSR-AR cells transduced with doxycycline-inducible constructs for the expression of NEK6 in male mice, with doxycycline maintained in the diet at time of harvest (+doxycycline) or with doxycycline diet removed 7 days prior to harvest (-doxycycline). Tumors were harvested 5 d after castration. C. Percentage of NEK6 positive cells (defined as having cytoplasmic NEK6 staining intensity greater than two standard deviations above the median) plotted against mean cytoplasmic NEK6 staining intensity (normalized as a percentile rank in each TMA) of cells within histologically benign glandular tissue (left) and tumor tissue (right) from radical prostatectomy specimens of patients with prostate cancer. Each point represents composite data from all benign or tumor cores from an individual patient. The threshold for positivity was set as the discontinuity in the distribution of % positive cells (at 12%) as indicated by the dashed red lines.

Supplemental Figure S3. A. Luciferase activity detected in LNCaP cells transiently transfected with an AR reporter either alone (top) or in combination with an expression plasmid for NEK6 (bottom) incubated with concentrations of the synthetic androgen R1881 indicated. B. Doxycycline-inducible expression of NEK6 wild-type, kinase dead (K74M/K75M), AKT1 and RAF1 both untagged and with C-terminal V5 tag. Untagged versions were used for experiments described. C. Inducible expression of NEK6 does not increase expression of AR targets PSA or TMPRSS2 in LHSR-AR cells. Expression of TMPRSS2 and PSA were measured by qPCR in the absence and presence of doxycycline to induce transgene expression and in the presence and absence of R1881 as indicated, with expression normalized to cells transduced with NEK6 K74M/K75M in the absence of doxycycline and R1881. D. NEK6 expression has neither a positive or negative effect on AR signaling as measured through published AR signatures. Gene expression changes conferred by inducible expression of wild-type NEK6 vs. kinase dead NEK6 six hours after growth factor stimulation were assayed in 3 biological replicates, and GSEA was used to assess enrichment of signatures positively correlated with AR activity in three data sets from the literature

Supplemental Figure S4. A. Immunohistochemistry of xenograft tumors derived from LHSR-AR cells transduced with doxycycline-inducible constructs for the expression of NEK6 in male mice, with doxycycline maintained in the diet at time of harvest (+doxycycline) or with doxycycline diet removed 7 days prior to harvest (-doxycycline). Tumors were harvested from non-castrated mice (day 0) or 2 or 5 days after castration. B. LHSR-AR cells expressing GFP or wild-type or mutant forms of NEK6 under a doxycycline inducible promoter, in the presence of doxycycline and absence of growth factor stimulation (lanes 1-4), with growth factor stimulation in the absence of doxycycline (lanes 5-9) and with growth factor stimulation in the presence of doxycycline (lanes 10-14). Immunoblots for phosphorylated forms of p70S6K at Thr412 and STAT3 at Ser727 demonstrate increases with growth factor stimulation (compare lanes 1-4 with lanes 10-14) but no increase in the presence of wild-type NEK6 (lanes 2, 12) as compared to kinase-dead NEK6 (lanes 1, 11). C. Immunoblots of protein lysates of xenograft tumors derived from LHSR-AR cells transduced with doxycycline-inducible constructs for the expression of GFP or NEK6 in male mice, with doxycycline maintained in the diet at time of harvest (+dox) or with doxycycline diet removed 7 days prior to harvest (-dox). Tumors were harvested from non-castrated mice (day 0) or 2 or 5 days after castration. Two exposures of the NEK6 immunoblot are shown, as well as immunoblots using antibodies specific to phosphorylated forms of p70S6K and STAT3 as shown. There is no consistent increased phosphorylation of these proteins in tumors expressing NEK6 (lanes 22-24) as compared to controls (lanes 19-21) in castrate conditions.

Supplemental Figure S5. NEK6 overexpression does not lead to promotion of cell cycle progression or antagonism of the p53 pathway in LHSR-AR cells. A. Cell cycle profiles of cells with and without NEK6 overexpression. LHSR-AR cells transduced with doxycycline-inducible NEK6 were cultured in the presence (bottom profiles) or absence (top profiles) of doxycycline, starved from growth factors for 24 hours, and released into growth factor-containing media for the times indicated, then harvested and fixed for propidium iodide staining in comparison to asynchronously cycling cells B. Proliferation curves of LHSR-AR constitutively expressing lacZ or NEK6, average cell counts from 3 plates collected at the indicated time points plotted compared to previous time point with standard deviations. C. p53 pathway is inactive in LHSR-AR cells, and NEK6 expression does not rescue from cell death mediated by etoposide. LHSR-AR cells with constitutive expression (pLX304-) of lacZ vs. NEK6 or doxycycline-inducible expression (pTRIPz-) of NEK6 kinase dead (kd) vs. wild-type (wt) were exposed to etoposide at concentrations indicated vs. DMSO as vehicle control. Attached and floating cells were harvested and combined for immunoblotting.

Supplemental Figure S6. A. Immunohistochemistry of xenograft tumors derived from LHSR-AR cells transduced with doxycycline-inducible constructs for the expression of NEK6 in male mice, with doxycycline maintained in the diet at time of harvest (+dox) or with doxycycline diet removed 7 days prior to harvest (-dox). Tumors were harvested from non-castrated mice (day 0) or 2 or 5 days after castration and stained by an antibody specific to KRT13.

Supplemental Table S1.

AR staining of transgene-mediated androgen-independent LHSR-AR xenografts

		AR Nuclear % score (0,1,2,3,4)[a]	AR Nuclear intensity[b]	AR % Cytoplasm score (0,1,2,3,4)[a]	AR Cytoplasm intensity[b]	notes
Male mice (pos control)	GFP 1 (one piece)	4	m **s**	3	w **m**	9.11.12
	GFP 1 (second piece)	3	w **m** s	1	w	
	GFP 2	4	m s	1	w	
	GFP 3	4	s	4	m s	
Female mice	NEK6 1 (one piece)	2	m **s**	2	w m	
	NEK6 2 (few pieces)	1	w	1	w	
	NEK6 3	trace	most nuclei are neg; occasional nuclei show weak staining (<1-2%)	trace	most cytoplasm are neg; occasional cells show weak staining (<1-2%)	surface mouse skin is neg for AR
	AKT1	2	m **s**	3	w **m** s	
	CCL2	0 (very small sample)	0	0 (very small sample)	0	scant epithelial cells
	ERBB2	2	**w** m s	2	w m	
	KRASV12 1 (one piece)	0		0		
	KRASV12 2 (2 other pieces)	1	**m** s	2	w **m**	
	MEKDD	1	w	4	**w** m s	
	PIM1	<5%	w (rare strong, 3-4 cells)	2	m **s**	
	RAF1	1	w m	4	w **m**	two pieces show this staining pattern; third piece has weak cyto stain in <25%, and nuclear stain weak in <25%.
Castrated mice	NEK6 castr	most are neg; however, one tissue fragment shows up to 3+ Nuc score in ~25% of nuclei	0-3			

[a] AR % score: 0, 1(1-25%),2(25-50%), 3(50-75%), 4(75-100%)

[b] Intensity: w=Weak, m=Moderate, s=Strong (**bold** indicates predominant intensity)

Supplemental Table S2
GO terms for NEK6 upregulated genes Day 5 after castration (filtered for >10 GeneHits)

GOID	GOTERM	Level	PVALUE	E Value	GeneHits
GO:0009607	response to biotic stimulus	3	0.000488	2.3	20
GO:0051707	response to other organism	3	0.000721	2.28	19
GO:0043207	response to external biotic stimulus	4	0.000721	2.28	19
GO:0051346	negative regulation of hydrolase activity	6	0.001169	2.84	12
GO:0050896	response to stimulus	2	0.002757	1.22	116
GO:0052548	regulation of endopeptidase activity	7	0.003788	2.59	11
GO:0006950	response to stress	3	0.004668	1.39	57
GO:0052547	regulation of peptidase activity	6	0.005497	2.46	11
GO:0097190	apoptotic signaling pathway	5	0.005583	2.1	15
GO:0098542	defense response to other organism	4	0.00694	2.38	11
GO:0043086	negative regulation of catalytic activity	5	0.008077	1.91	17
GO:0007010	cytoskeleton organization	4	0.008394	1.79	20
GO:0019221	cytokine-mediated signaling pathway	6	0.008509	2.32	11
GO:0006955	immune response	3	0.009865	1.61	27
GO:0009617	response to bacterium	4	0.011655	2.21	11
GO:0051704	multi-organism process	2	0.011946	1.46	37
GO:0030855	epithelial cell differentiation	6	0.018286	1.93	13
GO:0044699	single-organism process	2	0.018825	1.09	171
GO:0006952	defense response	4	0.019519	1.52	27
GO:0030162	regulation of proteolysis	6	0.021277	1.95	12

Supplemental Table S3.

A. The intersection of genes downregulated by castration in control tumors and upregulated by NEK6 overexpression after castration

PRG2	SNCG	KRT8	PLEKHG2	RP4-639F20.1
DISP1	PLAC8	KRT18	FXYD5	PRAF2
RP5-977B1.11	SH2B2	SLX1B	PDLIM1	SERPINB6
COPS7B	CKLF-CMTM1	ISG15	RP11-195F19.5	AC006538.1
RP11-473M20.7	RP13-638C3.4	C4B	MUC16	RPS2P7
UBE2D4	TPK1	AP001347.6	SAA2	MAP1S
CTD-2007L18.5	RP11-807G9.2	C19orf21	MVP	AC112229.7
CASKIN1	TMX4	A4GALT	HSPH1	RHOC
CINP	C10orf10	LY6E	BST2	IFI6
RP11-253M7.1	WFDC2	SCHIP1	RP11-961A15.1	UBXN11
PAX8	SNX24	AC009133.12	ISG20	RPL23AP7
SULT1A3	RP11-157P1.4	CFB	IRF7	NME4

B. GO terms intersection of Castration Down (Day 2 to 5) and NEK6 s/p castration Day 5 Up

GOID	GOTERM	Level	PVALUE	E Value	GeneHits
GO:0019221	cytokine-mediated signaling pathway	6	0.00002	8.18	7
GO:0060337	type I interferon signaling pathway	7	0.000023	23.98	4
GO:0071357	cellular response to type I interferon	6	0.000023	23.98	4
GO:0034340	response to type I interferon	5	0.000024	23.67	4
GO:0034097	response to cytokine	5	0.000041	6.06	8
GO:0051707	response to other organism	3	0.000099	5.34	8
GO:0043207	response to external biotic stimulus	4	0.000099	5.34	8
GO:0071345	cellular response to cytokine stimulus	6	0.000104	6.29	7
GO:0010951	negative regulation of endopeptidase activity	8	0.000107	10.5	5
GO:0010466	negative regulation of peptidase activity	7	0.000127	10.13	5

Supplemental Table S4.

A. Phoshphopeptides significantly enriched (q<0.25) in cell lysates with doxycycline-induced wild-type NEK6 expression as compared to lysates from cells expressing kinase-dead (kd) NEK6 and as compared to uninduced

Gene Name	Site	q enriched (wt vs. kd)	q enriched (wt induced vs. uninduced)	modifiedsequence_localization
LIMCH1	S303	9.73E-64	1.72E-102	_SWSTATS(ph)PLGGERPFR_7
DROSHA	S357	7.81E-32	2.87E-68	_NTDSWAPPLEIVNHRS(ph)PS(ph)REK_18
FOXJ2	S8	4.12E-18	2.22E-06	_(ac)ASDLESS(ph)LTSIDWLPQLTLR_7
FOXO3	S7	1.06E-17	4.06E-54	_(ac)AEAPAS(ph)PAPLSPLEVELDPEFEPQSRPR_6
HUWE1	S2595	7.84E-13	1.09E-09	_LLGPSAAADILQLSSS(ph)LPLQSR_16
EPPK1	S1529	4.20E-12	2.03E-06	_QVS(ph)ARDLFR_3
COIL	S487	6.79E-12	1.13E-13	_KIDS(ph)PPIRR_4
SRGAP1	S932	6.79E-12	1.21E-25	_LLELTS(ph)SYSPDVSDYKEGR_7
SLC2A12	S244	6.95E-11	2.89E-05	_LRALS(ph)DTTEELTVIK_5
TRPS1	S843	2.12E-09	3.99E-13	_TLRDS(ph)PNVEAAHLARPIYGLAVETK_5
MTX1	S9	4.78E-06	3.80E-03	_(ac)MLLGGPPRS(ph)PR_9
OGFR	S349	9.83E-06	9.02E-07	_S(ph)VEPQDAGPLER_1
INTS3	S502	5.00E-05	2.61E-06	_FPEFCSSPS(ph)PPVEVK_9
TRA2B	S239	7.67E-05	3.27E-03	_S(ph)YRGGGGGGGWR_1
LMO7	S926	9.02E-05	5.17E-02	_GISS(ph)LPR_4

SATB2	S20	9.20E-05	5.42E-02	_SGS(ph)PDVKGPPPVK_3
ATM	T1885	1.32E-04	1.83E-02	_STT(ph)PANLDSESEHFFR_3
PLEKHA6	S313	3.42E-04	2.86E-06	_KSS(ph)MNQLQQWVNLRR_3
LMO7	S895	3.62E-04	2.13E-01	_VSAS(ph)LPR_4
PAK6	S246	4.80E-04	8.11E-07	_HGSEEARPQSCLVGSATGRPGGEGS(ph)PS(ph)PK_25
HNRNPM	S633	6.05E-04	3.70E-04	_GNFGGS(ph)FAGSFGGAGGHAPGVAR_6
MLLT3	S302	2.20E-03	9.42E-02	_KKS(ph)SSEALFK_3
HNRNPA2B1	S324	2.41E-03	5.43E-03	_SGNFGGS(ph)RNMGGPYGGGNYGPGGSGGSGGYGGR_7
NCOA5	S96	2.52E-03	1.18E-01	_DLRDS(ph)RDFR_5
SETX	T2474	2.53E-03	1.92E-01	_SLT(ph)HPPTIAPEGSRPQGGLPSSKLDSGFAK_3
BCL6	S466	2.65E-03	2.40E-01	_SSSESHS(ph)PLYMHPPK_7
ATXN1	S811	2.94E-03	1.27E-03	_ICIEGRS(ph)NVGK_7
CDKN2AIP	S151	3.23E-03	1.47E-01	_VIEGKNS(ph)SAVEQDHAK_7
FAM21C	S288	3.49E-03	1.82E-01	_S(ph)RPTS(ph)FADELAAR_5
EPS8L1	T305	5.41E-03	3.80E-02	_AAGEGLLT(ph)LR_8
FOXA1	S307	5.42E-03	1.00E-01	_KDPSGASNPSADS(ph)PLHR_13
KLF4	T316	6.40E-03	6.99E-05	_TT(ph)PTLGLEEVLSSR_2
LMO7	S1593	6.56E-03	1.32E-02	_SHS(ph)PSASQSGSQLR_3
ZNF326	S131	8.20E-03	1.57E-01	_NQGGSS(ph)WEAPYSR_6
PLEKHG6	S645	2.05E-02	1.29E-02	_S(ph)APELPEGILK_1
RIPK3	S316	3.04E-02	1.70E-03	_RFS(ph)IPESGQGGTEMDGFRR_3
ZNF326	S106	3.98E-02	9.73E-09	_FGGS(ph)YGGRFESSYR_4
ERCC5	S156	4.94E-02	1.03E-01	_ENDLYVLPPLQEEEKHS(ph)S(ph)EEEDEKEWQER_17
ERCC5	S157	4.94E-02	1.03E-01	_ENDLYVLPPLQEEEKHS(ph)S(ph)EEEDEKEWQER_18
LIG1	S66	5.02E-02	9.97E-02	_VLGS(ph)EGEEEDEALS(ph)PAK_4
MYOF	S193	5.29E-02	9.46E-04	_RMLS(ph)NKPQDFQIR_4
ZDHHC18	S19	6.19E-02	1.13E-07	_(ac)MKDCEYQQISPGAAPLPAS(ph)PGAR_19
PBRM1	S353	6.53E-02	1.45E-09	_LSAITM(ox)ALQYGS(ph)ES(ph)EEDAALAAAR_12
EXPH5	S1444	7.11E-02	3.82E-02	_RSS(ph)WECTGSGR_3
SIPA1L3	S158	7.11E-02	5.33E-07	_SKDVEFQDGWPRS(ph)PGR_13
ATXN1	S238	7.85E-02	9.85E-02	_APGLITPGS(ph)PPPAQQNQYVHIS(ph)SSPQNTGR_9
KRT18	S323	8.16E-02	1.44E-01	_NLKASLENS(ph)LREVEAR_9
IRF2BP1	S453	9.61E-02	4.17E-02	_NVAEALGHSPKDPGGGGGPVRAGGAS(ph)PAASSTAQPPTQHR_26
DLG3	Y673	1.01E-01	1.62E-01	_RDNEVDGQDY(ph)HFVVSR_10
ATXN1	S775	1.02E-01	7.46E-03	_WS(ph)APESR_2
EXPH5	S341	1.12E-01	3.01E-02	_S(ph)LHFPATTQSK_1
RFX2	S28	1.27E-01	2.98E-02	_(ac)MQNSEGGADSPASVALRPSAAAPPVPAS(ph)PQR_28
PCYT1B	S315	1.59E-01	3.42E-02	_M(ox)LQALS(ph)PK_6
EPS8L1	T202	1.61E-01	2.35E-01	_AVIST(ph)VER_5
HIVEP2	S2300	1.81E-01	3.82E-02	_RGPHALQSSGPPSTPS(ph)SPR_17
ZNF608	S964	1.96E-01	4.92E-05	_SKASS(ph)PSDIISSKDSVVK_5
KLF3	S71	2.08E-01	2.39E-23	_S(ph)SPPSAGNSPSSLKFPSSHRR_2
ACLY	S481	2.24E-01	2.45E-04	_KAKPAMPQDSVPS(ph)PR_13
ZNF608	S1453	2.31E-01	4.83E-07	_DRHS(ph)PFGQR_4

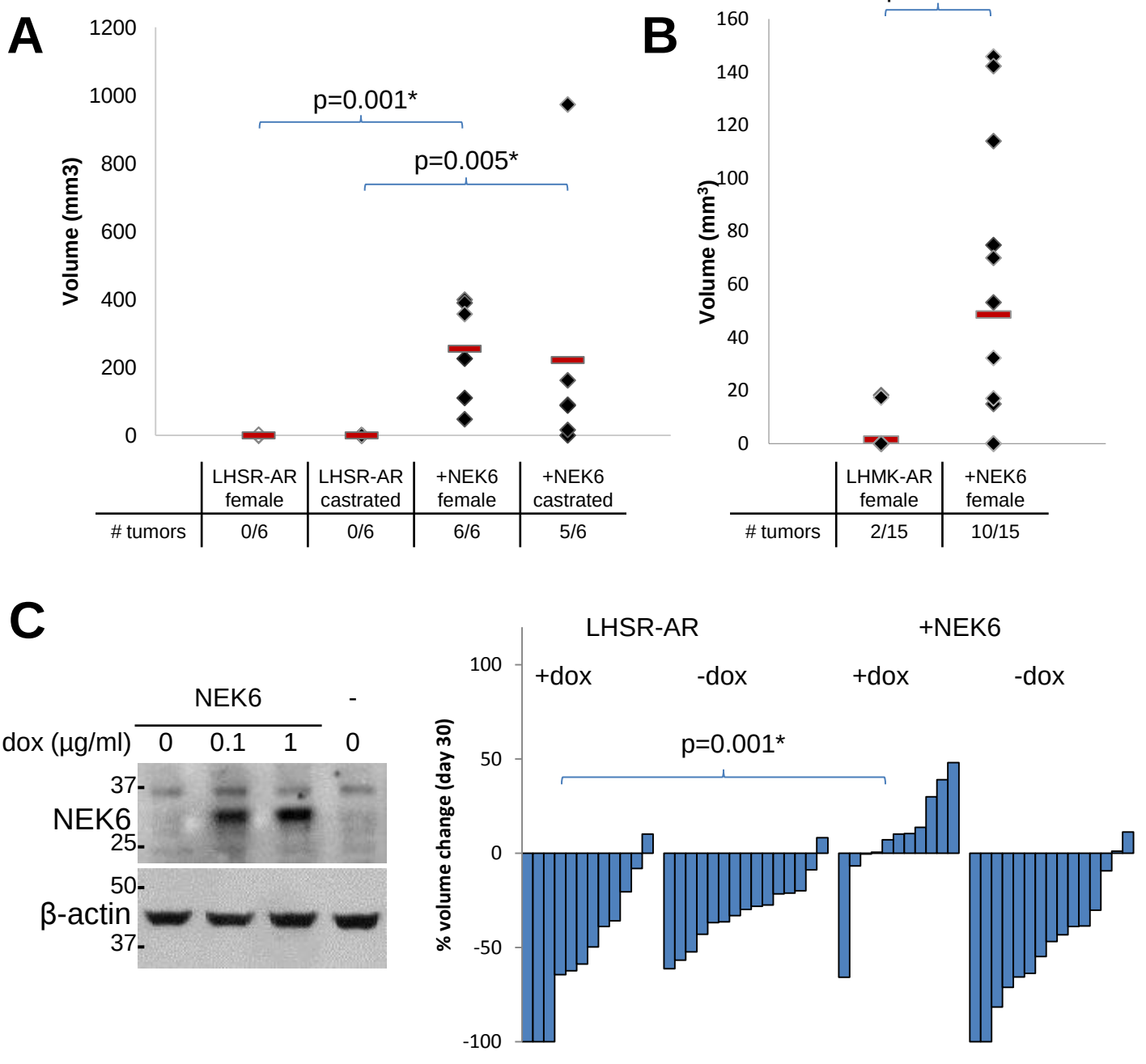
A
Volume (mm3)
1200
1000
800
600
400
200
0
p=0.001*
p=0.005*
LHSR-AR female
LHSR-AR castrated
+NEK6 female
+NEK6 castrated
tumors
0/6
0/6
6/6
5/6
B
Volume (mm³)
160
140
120
100
80
60
40
20
0
p=0.034*
LHMK-AR female
+NEK6 female
tumors
2/15
10/15
C
NEK6
-
dox (µg/ml)
0
0.1
1
0
37
NEK6
25
50
β-actin
37
LHSR-AR
+NEK6
+dox
-dox
+dox
-dox
100
50
0
-50
-100
% volume change (day 30)
p=0.001*

Figure 1

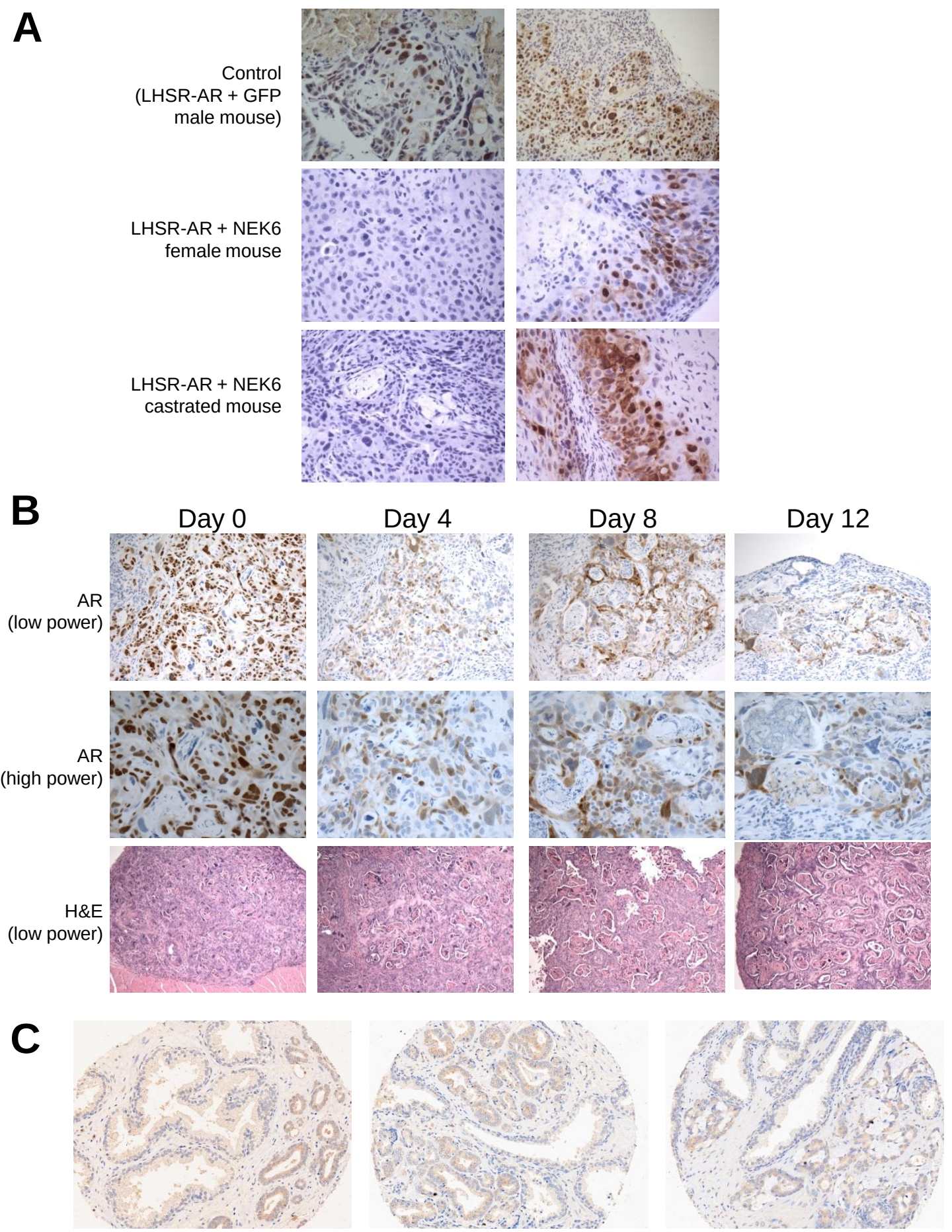
A
Control
(LHSR-AR + GFP
male mouse)
LHSR-AR + NEK6
female mouse
LHSR-AR + NEK6
castrated mouse
B
Day 0
Day 4
Day 8
Day 12
AR
(low power)
AR
(high power)
H&E
(low power)
C

Figure 2

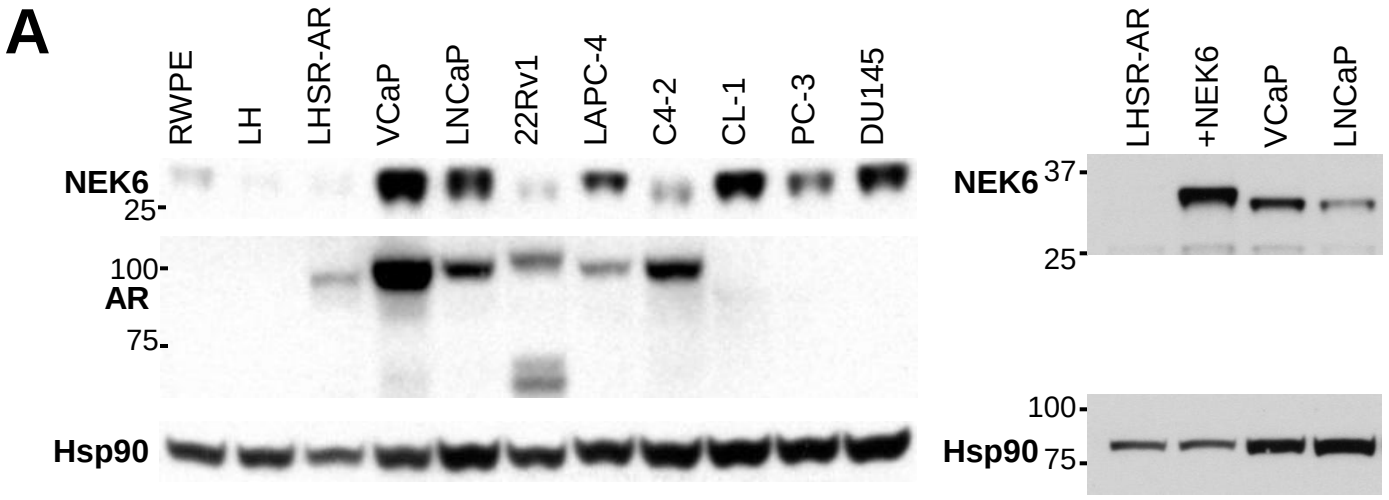
A
RWPE
LH
LHSR-AR
VCaP
LNCaP
22Rv1
LAPC-4
C4-2
CL-1
PC-3
DU145
NEK6
25
100
AR
75
Hsp90
LHSR-AR
+NEK6
VCaP
LNCaP
NEK6
37
25
100
Hsp90
75

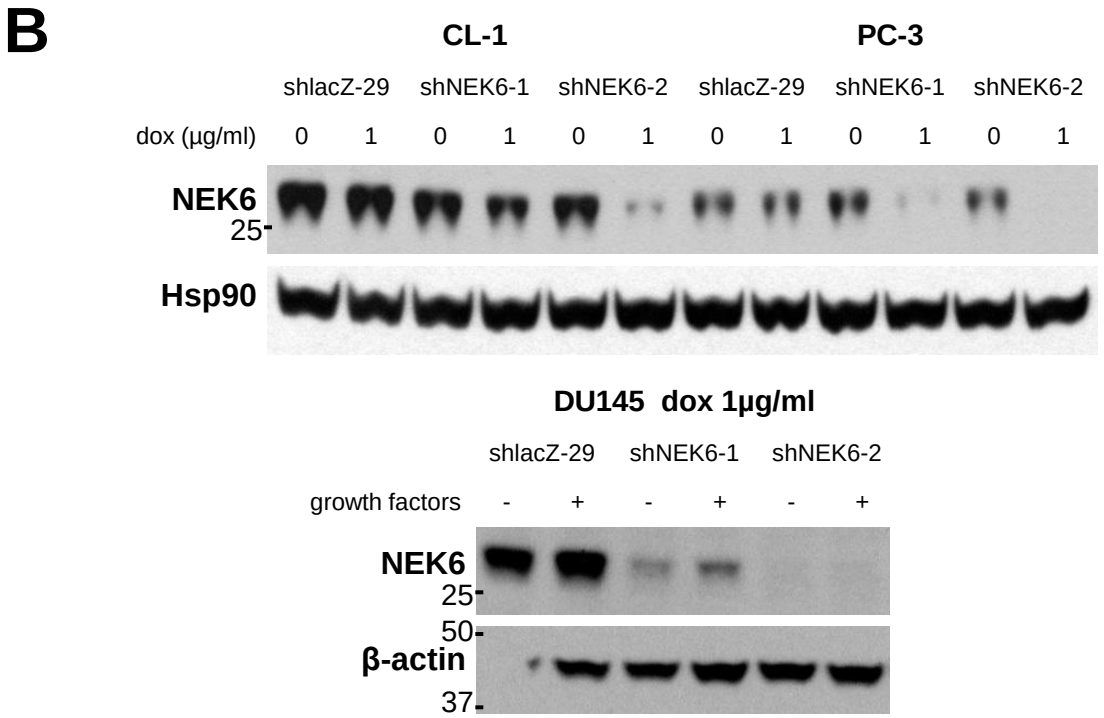
B
CL-1
PC-3
shlacZ-29
shNEK6-1
shNEK6-2
shlacZ-29
shNEK6-1
shNEK6-2
dox (µg/ml)
0 1 0 1 0 1 0 1 0 1 0 1
NEK6
25
Hsp90
DU145 dox 1µg/ml
shlacZ-29
shNEK6-1
shNEK6-2
growth factors
- + - + - +
NEK6
25
50
β-actin
37

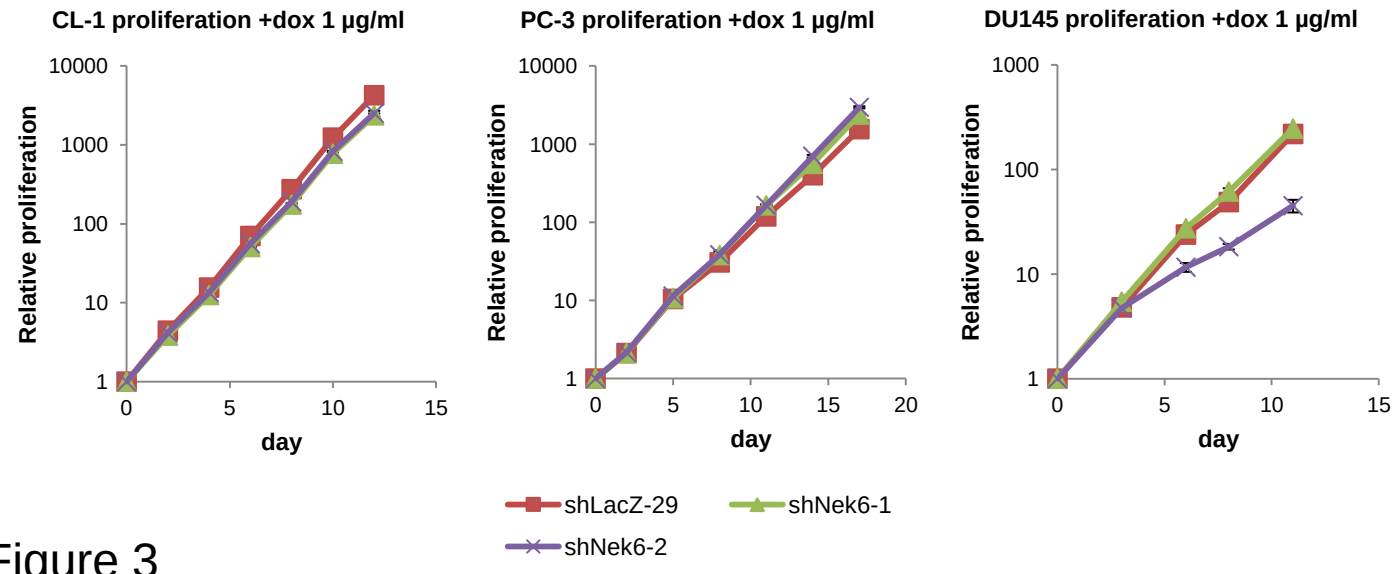
C
CL-1 proliferation +dox 1 µg/ml
PC-3 proliferation +dox 1 µg/ml
DU145 proliferation +dox 1 µg/ml
Relative proliferation
10000
1000
100
10
1
0
5
10
15
20
day
shLacZ-29
shNek6-1
shNek6-2

Figure 3

A

pTRIPz-GFP						pTRIPz-NEK6																	
day 0			day 2			day 0						day 2						day 5					
+dox						-dox			+dox			-dox			+dox			-dox			+dox		
1	2	3	1	2	3	1	2	3	1	2	3	1	2	3	1	2	3	1	2	3	1	2	3

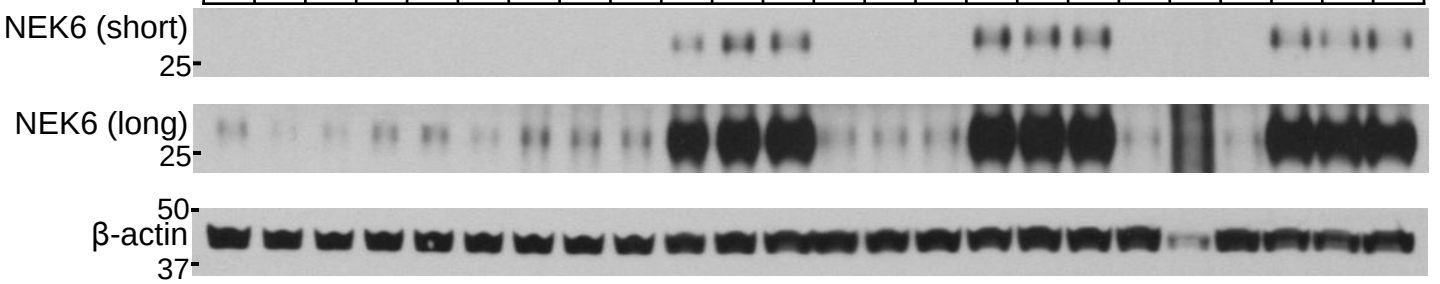

B

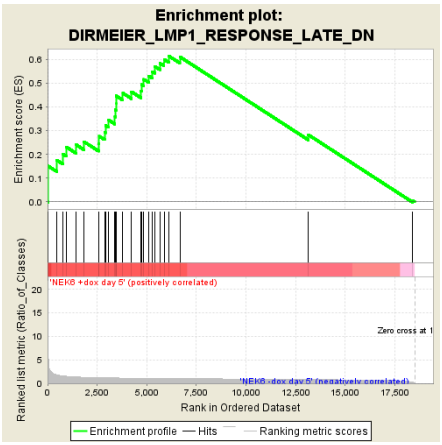

Enrichment Score (ES)	0.6142362
Normalized Enrichment Score (NES)	2.9263046
Nominal p-value	0.0
FDR q-value	7.961313E-4
FWER p-Value	0.001

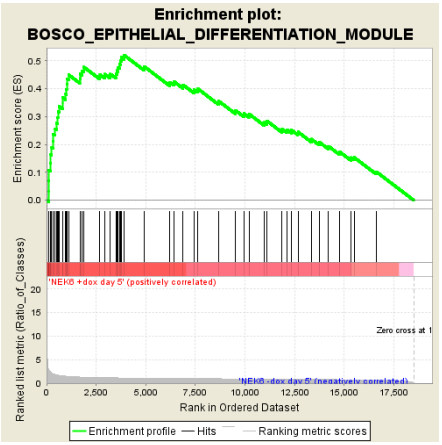

Enrichment Score (ES)	0.519851
Normalized Enrichment Score (NES)	2.9107523
Nominal p-value	0.0
FDR q-value	7.999157E-4
FWER p-Value	0.002

C

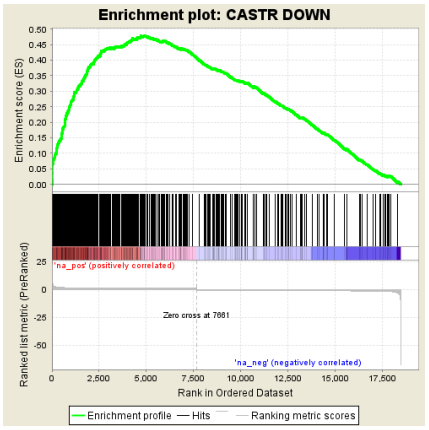

Enrichment Score (ES)	0.47908518
Normalized Enrichment Score (NES)	6.545397
Nominal p-value	0.0
FDR q-value	0.0
FWER p-Value	0.0

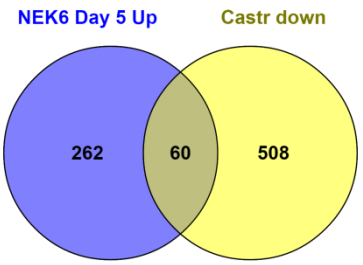

Figure 4

A

	L-X-X-pS/pT-F/W/Y/M/L/I/V/R/K (NEK6 general consensus)	L/F/W/Y-X-X-pS/pT-F/W/Y/M/L/I/V/R/K (NEK6 acceptable)	pS/pT-P (proline-directed kinases)	R-X-R-X-X-pS/pT (AKT1 or RSK family)	R-X-X-S (CaMK consensus)	pS/pT-D/E-X-D/E (CK2 consensus)	Others
Proteins with phosphopeptides meeting significance threshold (59 total phosphopeptides representing 50 proteins)	**FOXJ2** HUWE1 **NCOA5** KRT18	TRA2B (Y-X-X-pS-Y) HNRNPM (F-X-X-pS-F) HNRNPA2B1 (F-X-X-pS-F) ZNF326 (F-X-X-pS-Y)	Transcriptional modulators FOXO3 TRPS1 LMO7 SATB2 PAK6 BCL6 FOXA1 KLF4 ATXN1 IRF2BP1 RFX2 HIVEP2 KLF3 Others (x13)	SLC2A12 FAM21C ATXN1	PLEKHA6 RIPK3 MYOF EXPH5 MLLT3	ERCC5 LIG1 PBRM1	16 phosphopeptides representing 14 proteins 12 pS 3 pT 1 pY
Enrichment (compared to all detected phosphopeptides)	4/59 vs. 131/9362 (p=0.0092 Fisher's exact)	8/59 vs. 186/9362 ($p=1.95\times10^{-5}$)	26/59 vs. 4815/9434 (p=NS)	3/59 vs. 434/9301 (p=NS)	9/59 vs. 2239/9362 (p=NS)	3/59 vs. 701/9417 (p=NS)	

B

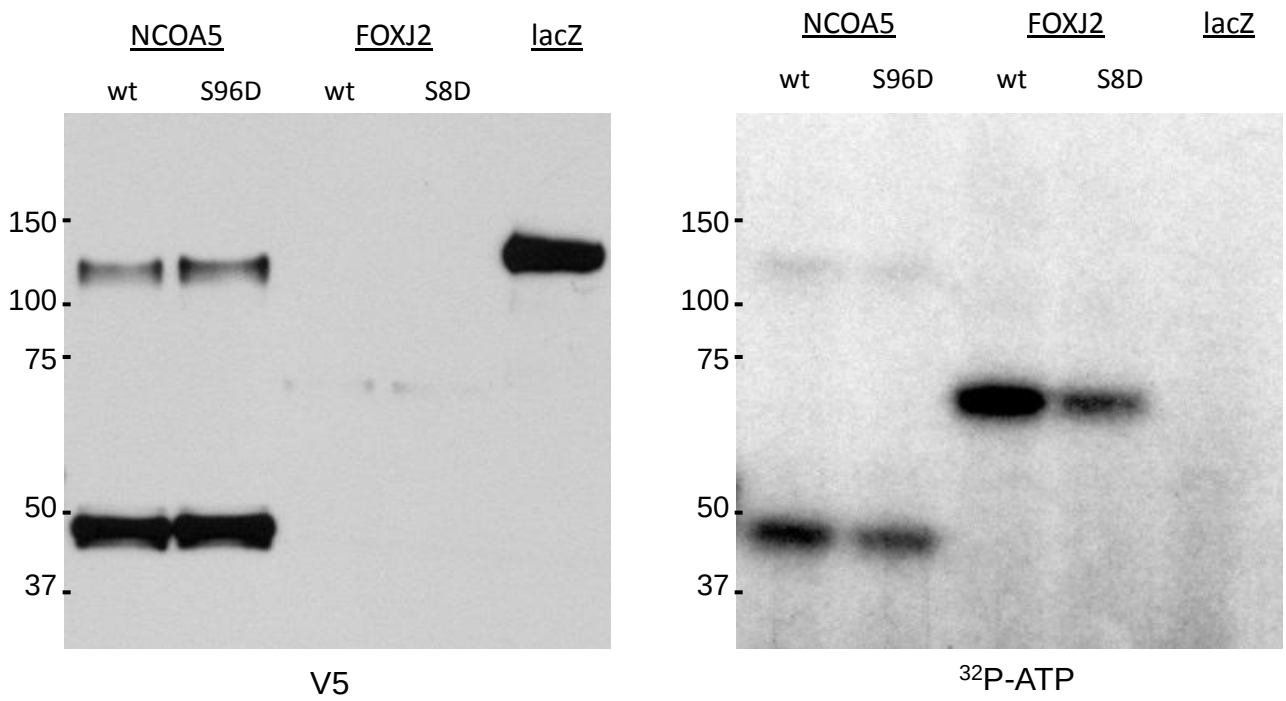

Figure 5

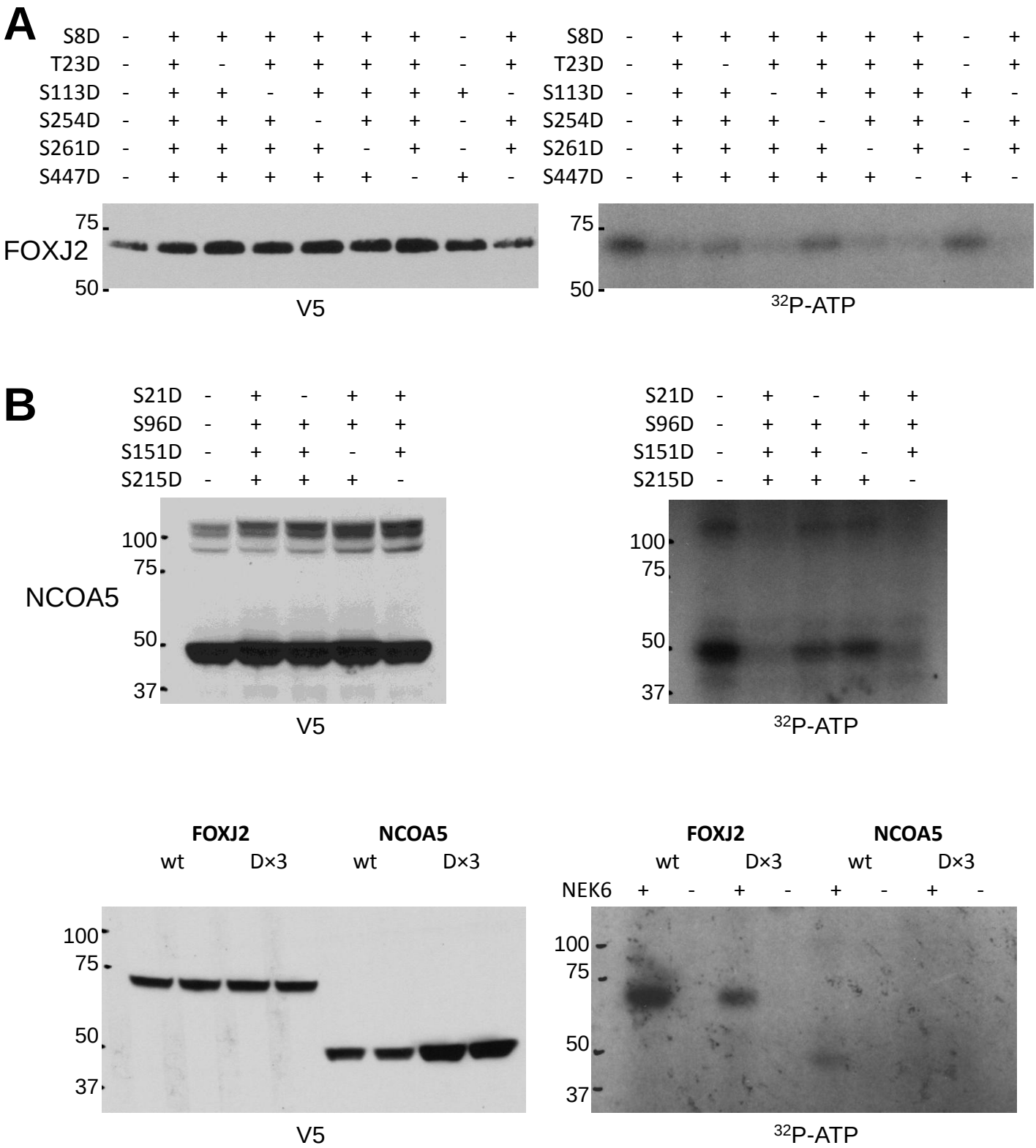
A
S8D - + + + + + + - +
T23D - + - + + + + - +
S113D - + + - + + + + -
S254D - + + + - + + - +
S261D - + + + + - + - +
S447D - + + + + + - + -
75
FOXJ2
50
V5
S8D - + + + + + + - +
T23D - + - + + + + - +
S113D - + + - + + + + -
S254D - + + + - + + - +
S261D - + + + + - + - +
S447D - + + + + + - + -
75
50
32P-ATP
B
S21D - + - + +
S96D - + + + +
S151D - + + - +
S215D - + + + -
100
75
NCOA5
50
37
V5
S21D - + - + +
S96D - + + + +
S151D - + + - +
S215D - + + + -
100
75
50
37
32P-ATP
FOXJ2
NCOA5
wt
D×3
wt
D×3
100
75
50
37
V5
FOXJ2
NCOA5
wt
D×3
wt
D×3
NEK6 + - + - + - + -
100
75
50
37
32P-ATP

Figure 6

A

Enrichment Score (ES)	0.21139549
Normalized Enrichment Score (NES)	2.6029801
Nominal p-value	0.0
FDR q-value	0.0015906681
FWER p-Value	0.001

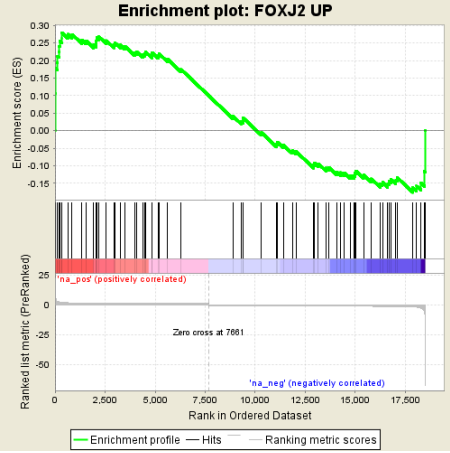

Enrichment Score (ES)	0.27894732
Normalized Enrichment Score (NES)	2.193419
Nominal p-value	0.002688172
FDR q-value	0.004374337
FWER p-Value	0.005

Enrichment Score (ES)	0.14760399
Normalized Enrichment Score (NES)	2.1382623
Nominal p-value	0.0
FDR q-value	0.005037116
FWER p-Value	0.01

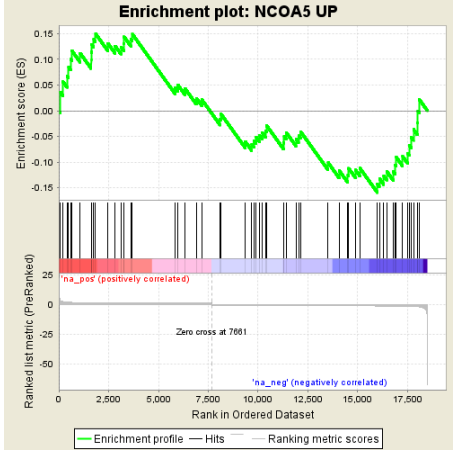

Enrichment Score (ES)	-0.15948276
Normalized Enrichment Score (NES)	-1.0333841
Nominal p-value	0.36886632
FDR q-value	0.4769835
FWER p-Value	0.913

B

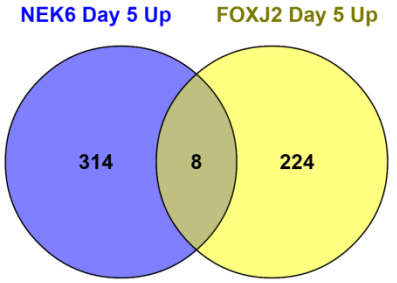

TPPP3
CRIP1
GSG1
PSCA
C14orf80
PLAC8
MAL
CCDC80

C

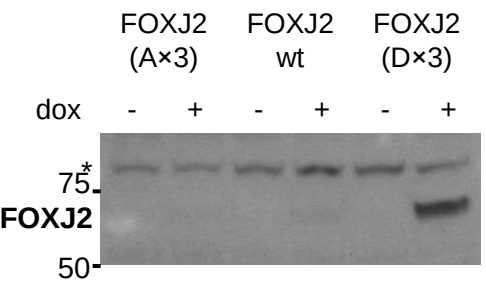

D

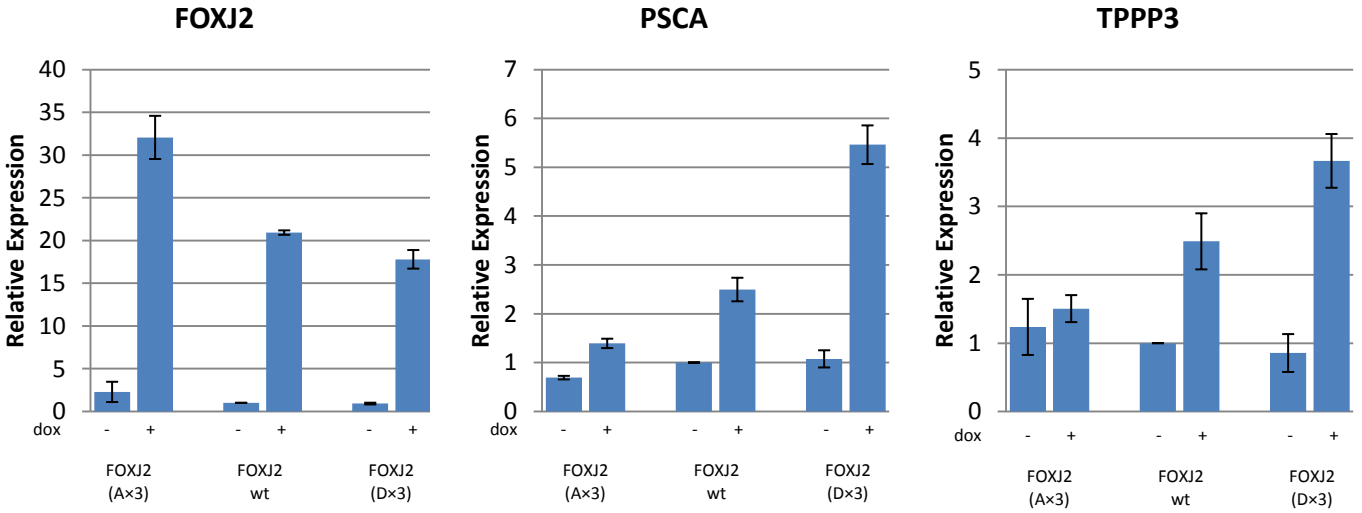

Figure 7

Positive selection screen

- Androgen-sensitive cell lines: **LNCaP**
- Pooled Screen With Lentiviral Library
- ~ 17,000 barcoded ORFs
- 1000 cells/ORF
- 3 conditions
- 3 technical repeats in parallel
- ~30% infection rate; M.O.I. < 1 (34, 28, 26%)
- After 25 Days, Identify enriched barcodes

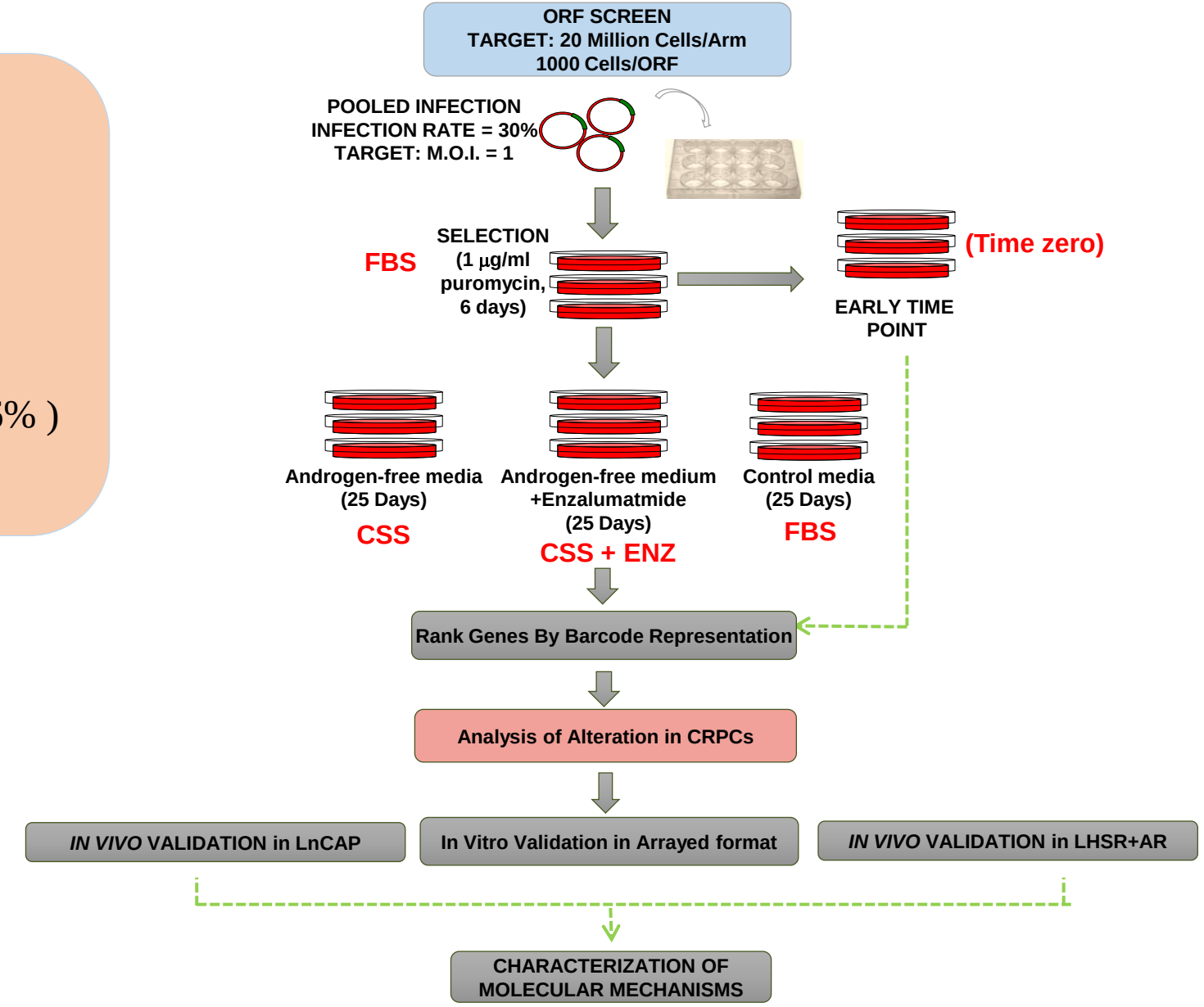

Figure 8

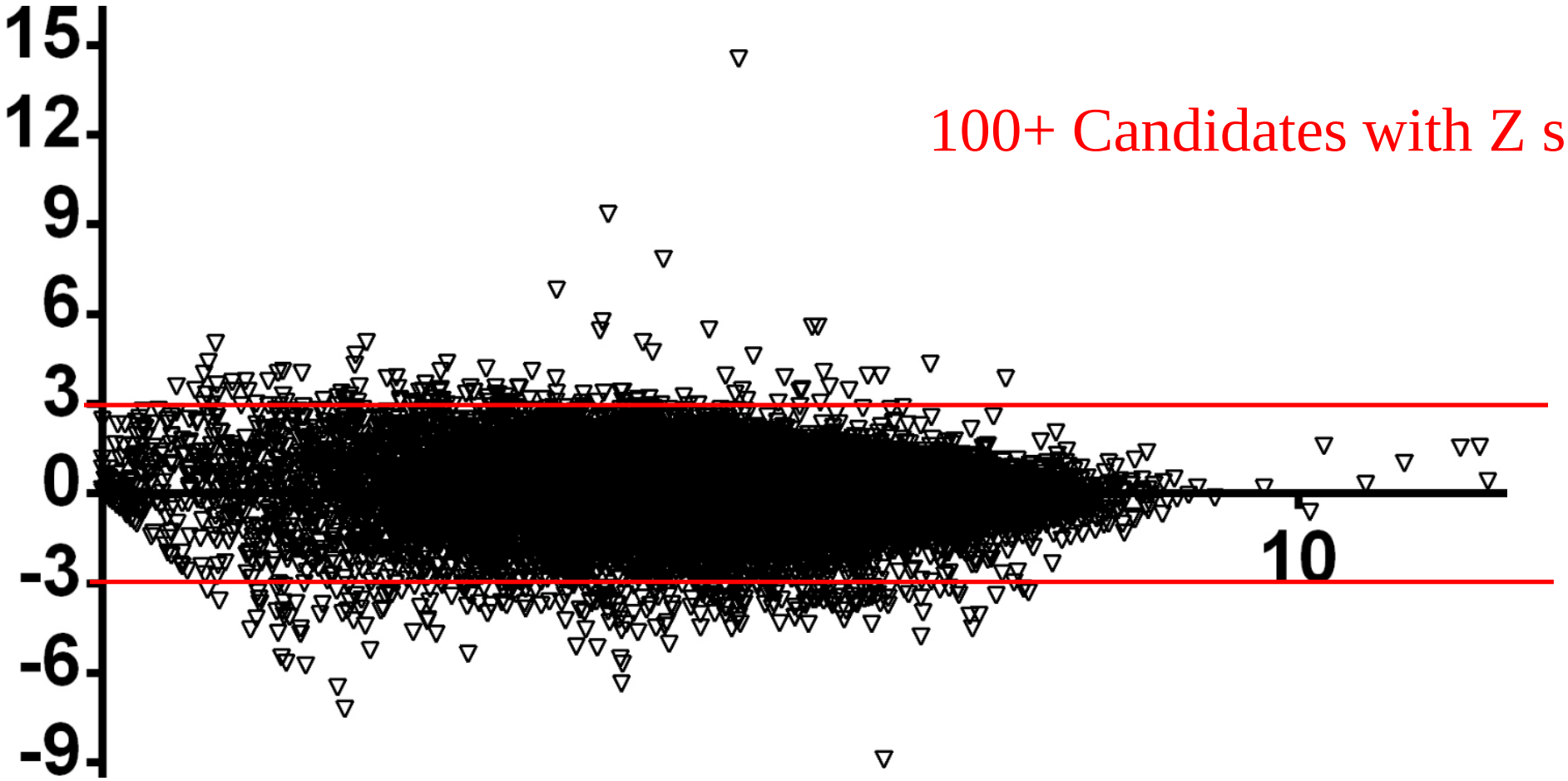

100+ Candidates with Z score > 3

Z score of 3 = 99.7 percentile or 3 standard deviations above mean;
ETV5, Z = 3.04; An ETS transcription factor implicated in CRPCs by GRASSO et al.

Figure 9

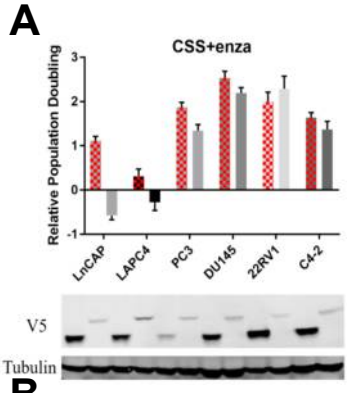

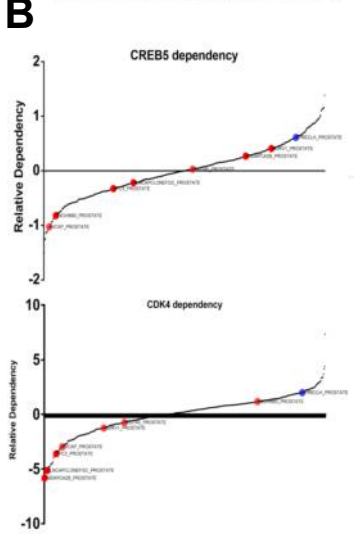

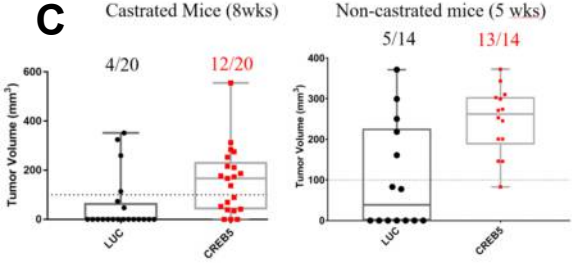

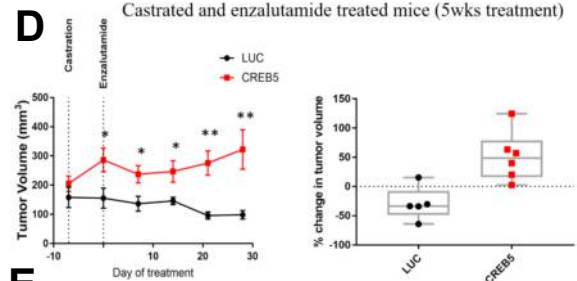

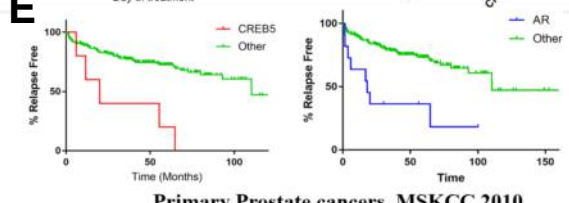

Primary Prostate cancers, MSKCC 2010

mRNA Z>2, 10 year relapse

	Relapsed	Median (Months)	P (Mantel-Cox)	Hazard Ratio	95% CI
CREB5	**5/5**	**20.4**	0.0003*	31.2	4.896 to 198.9
Other	55/136	110.3			
AR	**8/11**	**18**	0.0001*	13.94	3.689 to 52.65
Other	52/133	110.3			

*Hazard Ratio (Mantel-Haenszel)

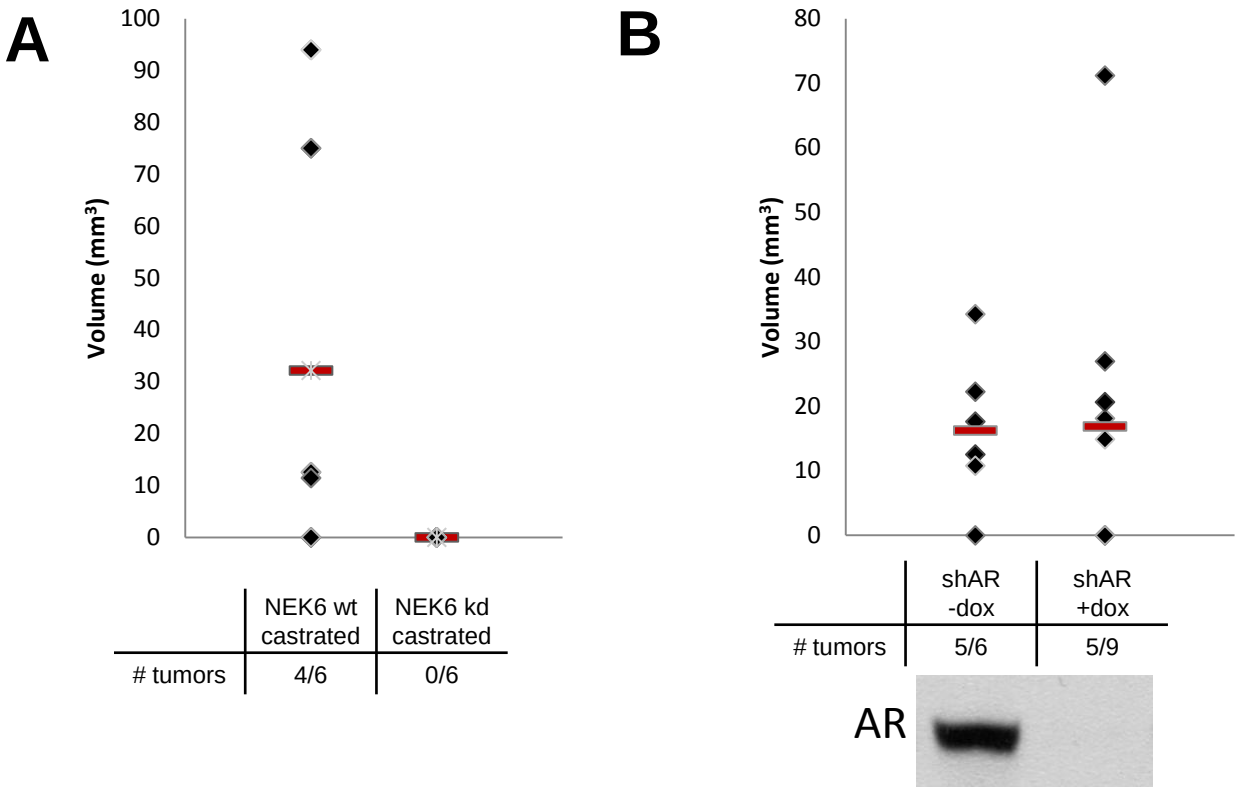

Supplemental Figure S1

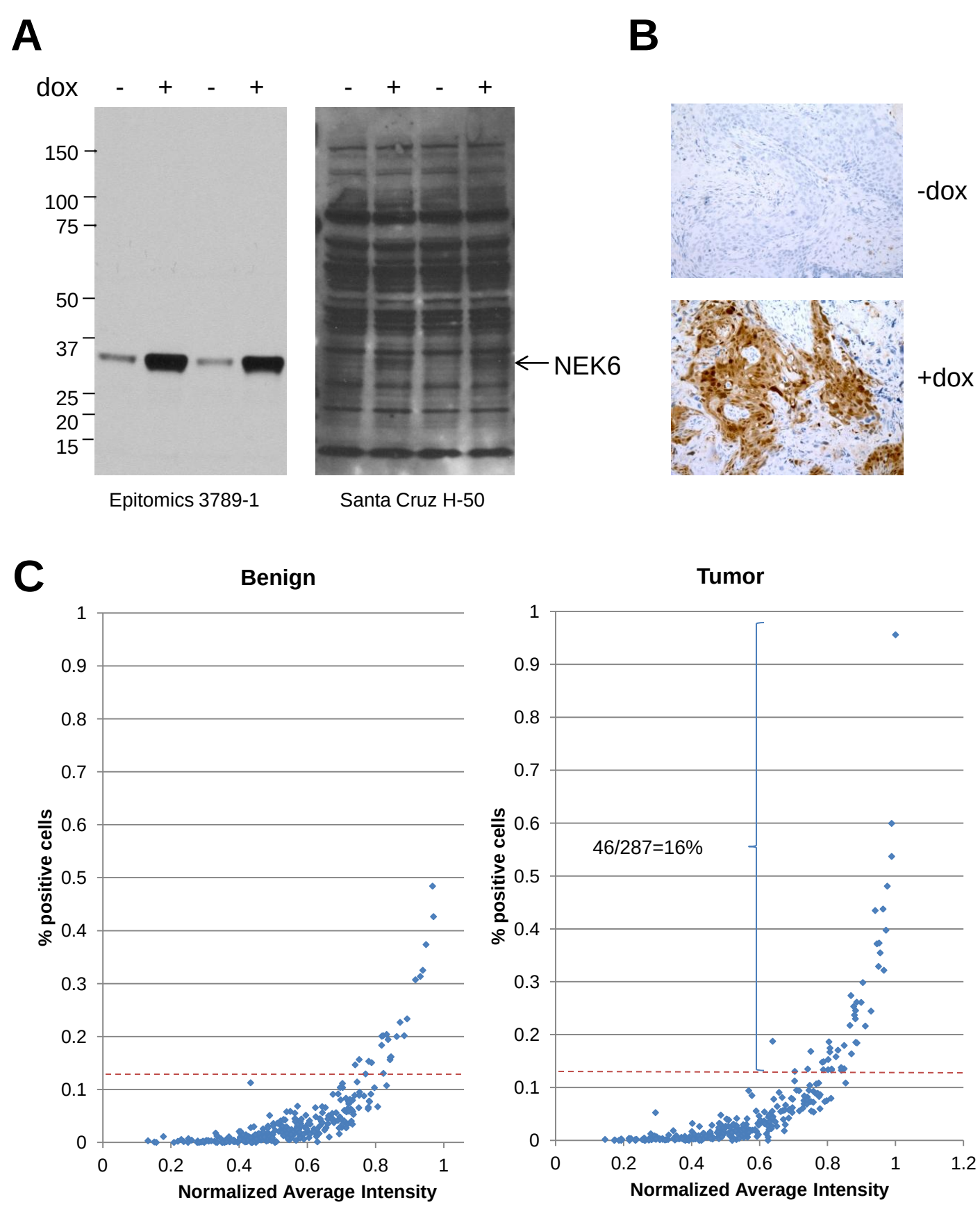

Supplemental Figure S2

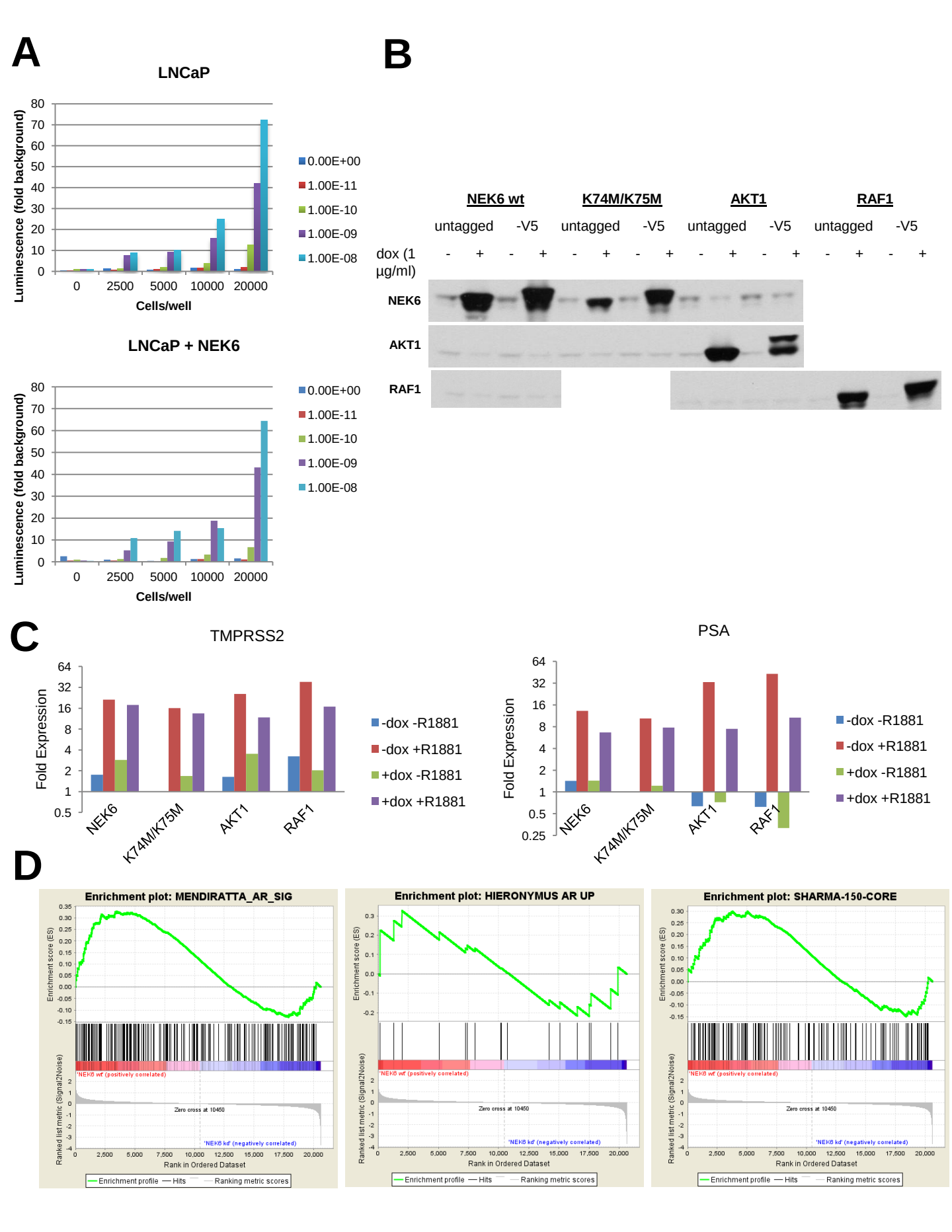

Supplemental Figure S3

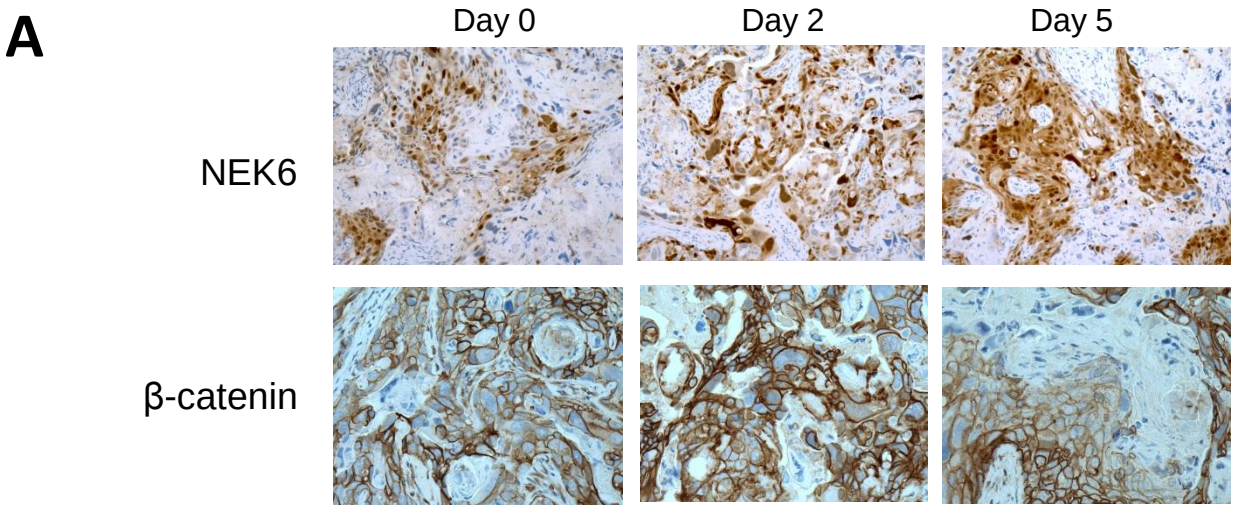

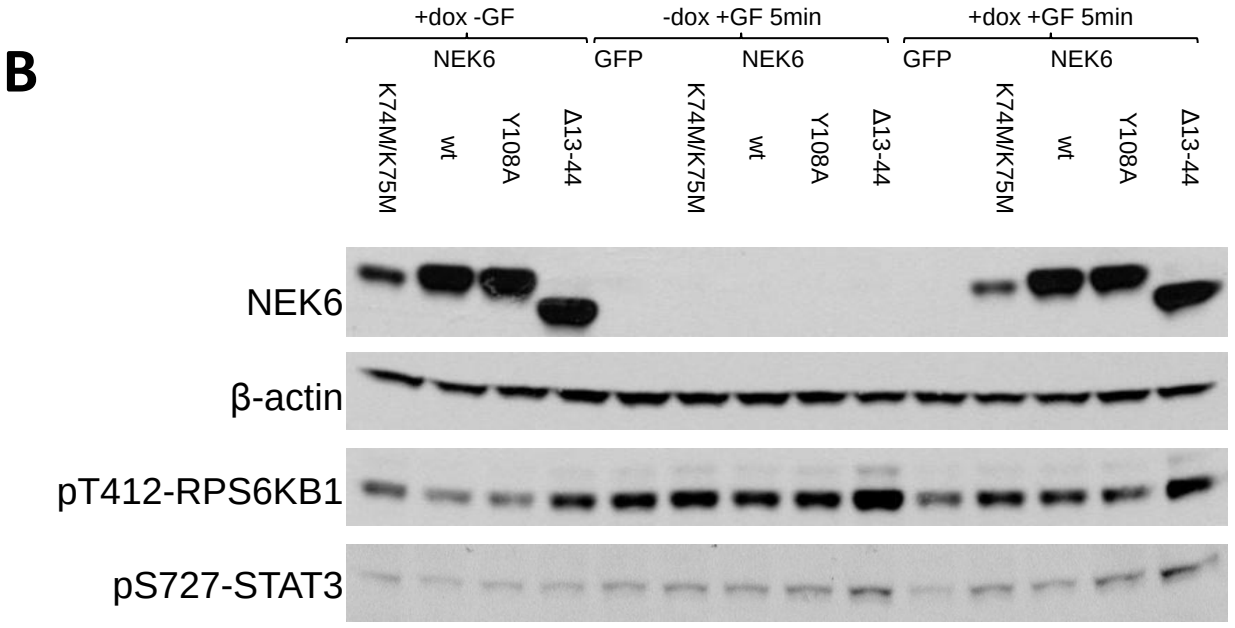

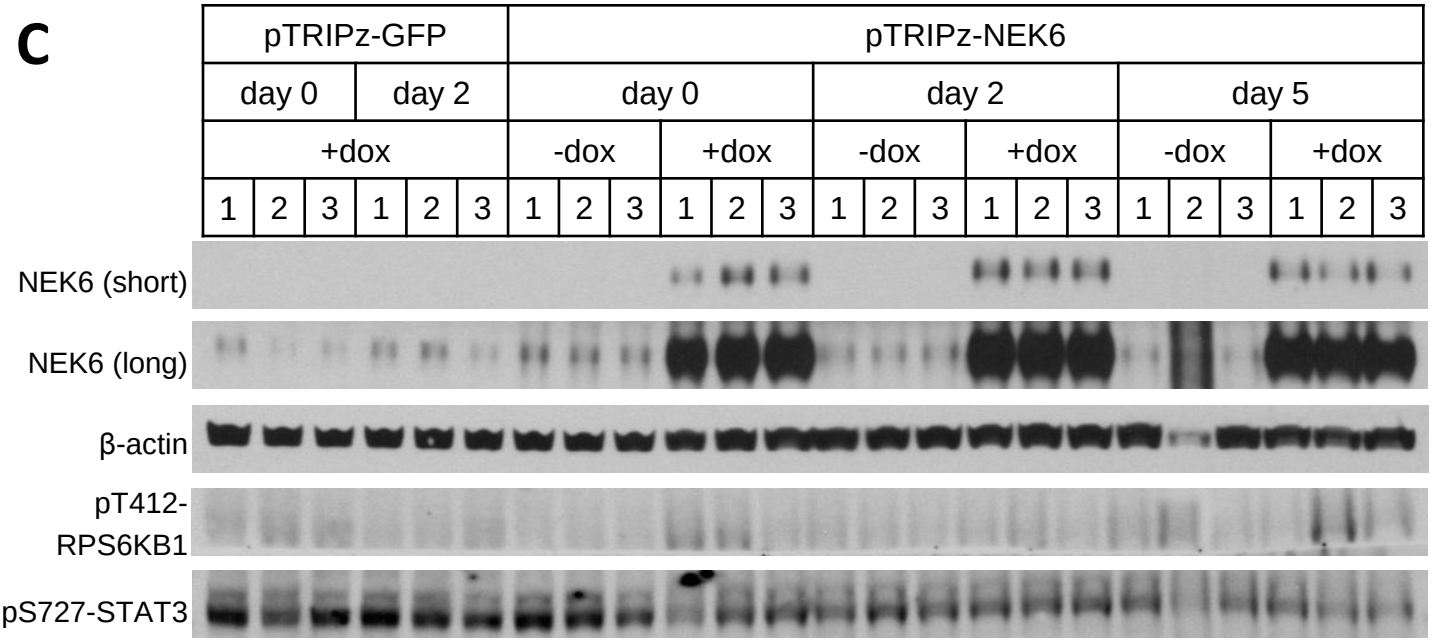

Supplemental Figure S4

A

-dox

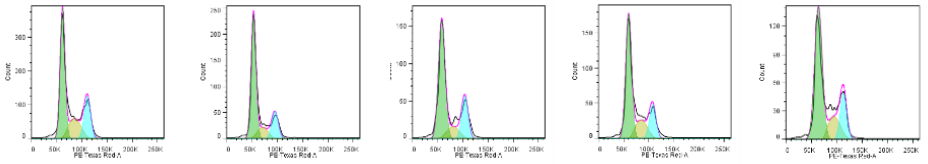

	async		0 h		4 h		8 h		24 h	
	-dox	+dox	-dox	+dox	-dox	+dox	-dox	+dox	-dox	+dox
G0/G1	54.5	54.2	69.2	67.8	58.9	57.1	57.6	51.6	51.6	50.9
S	15.5	16.2	8.4	7.1	13.6	13.1	16.9	16.9	19	17.8
G2/M	25	23.5	18.4	14.9	19.3	22.3	19.1	20	21.9	19.5
sub-G1	5.1	4.7	4.0	10.0	6.8	5.8	6.0	9.7	6.9	10

+dox

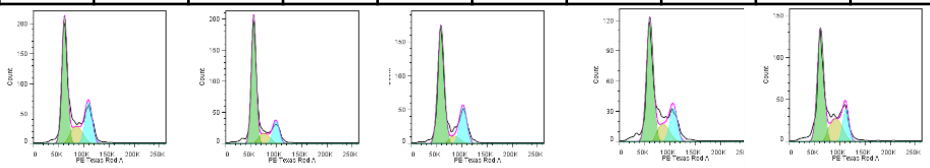

B

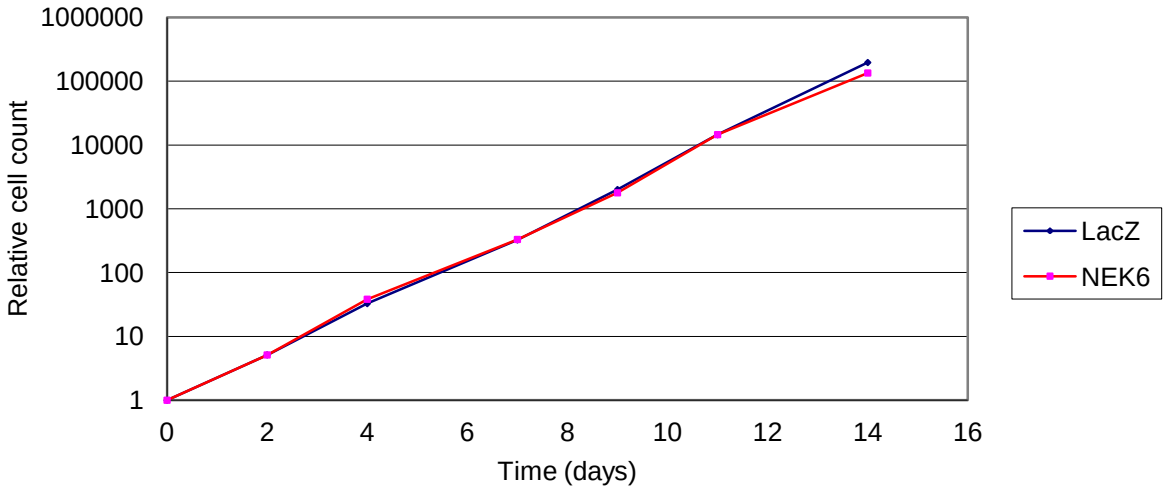

C

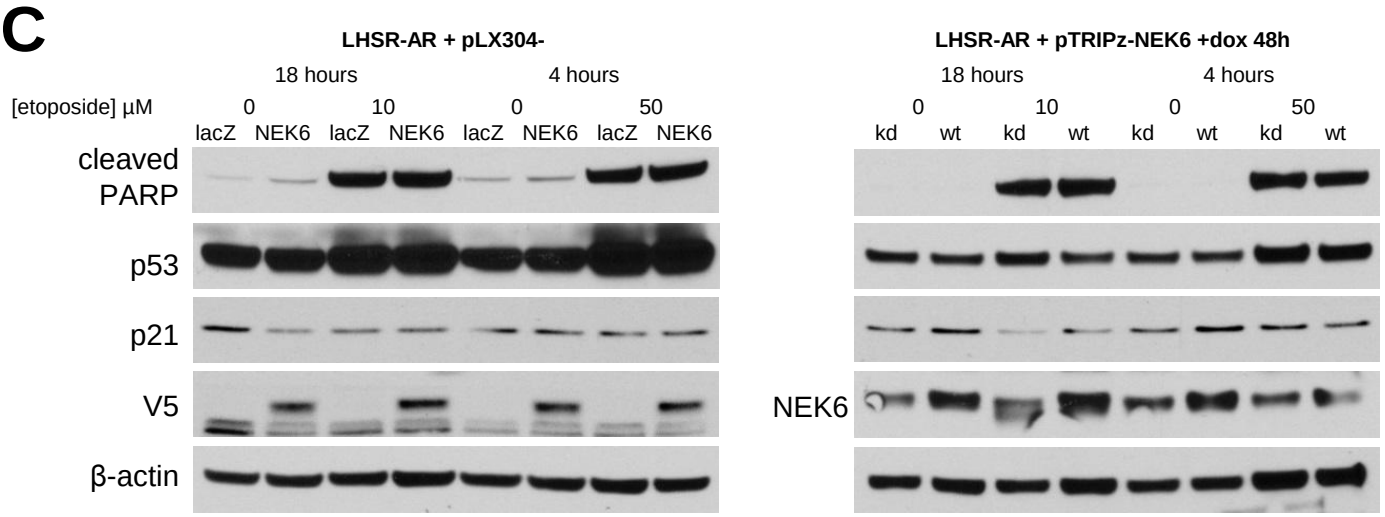

Supplemental Figure S5

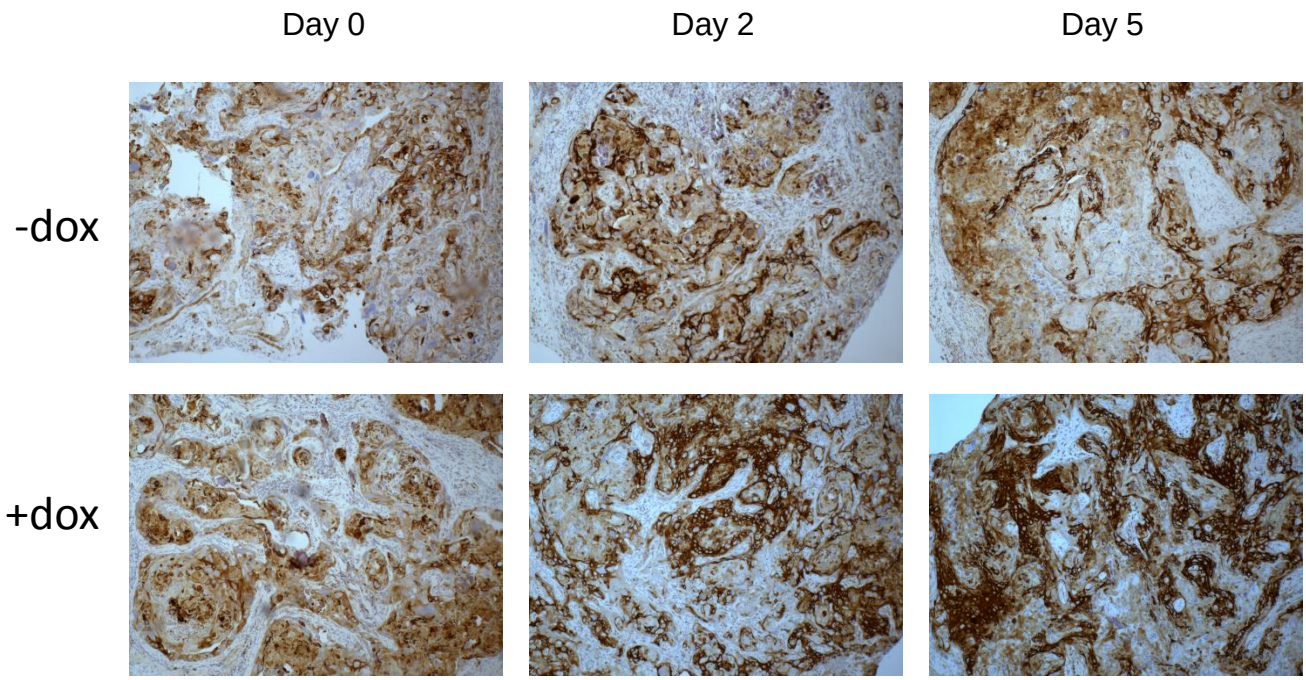

Supplemental Figure S6